PENSOFT

SENCKENBERG
world of biodiversity

Leibniz Association

Phylogeny, infrageneric classification and historical biogeography of *Mesochila* Rivalier, 1969 (Coleoptera: Cicindelidae), with the performance of different phylogenetic inferences using morphological data compared

André Silva Roza[1,2] Carlos G. Schrago[3], José Ricardo M. Mermudes[1]

1 *Laboratório de Entomologia, Departamento de Zoologia, Instituto de Biologia, Universidade Federal do Rio de Janeiro, A1–107, Bloco A, Av. Carlos Chagas Filho, 373, Cidade Universitária, Ilha do Fundão, Rio de Janeiro, Brazil; [andreroza1993@gmail.com], [jrmermudes@gmail.com]*

2 *Programa de Pós-graduação em Zoologia, Museu Nacional, Universidade Federal do Rio de Janeiro, Rio de Janeiro, RJ, Brazil*

3 *Laboratório de Biologia Evolutiva Teórica e Aplicada, Departamento de Genética, Instituto de Biologia, Universidade Federal do Rio de Janeiro, A2–092, Bloco A, 21941-617, Rio de Janeiro, RJ, Brazil; [carlos.schrago@gmail.com]*

http://zoobank.org/AAE97520-88C7-42EC-ADA1-2F4030F2DBA6

Corresponding author: André Silva Roza (andreroza1993@gmail.com)

Received 14 October 2021
Accepted 4 February 2022
Published 20 May 2022

Academic Editors André Nel, Marianna Simões

Citation: Roza AS, Schrago CG, Mermudes JRM (2022) Phylogeny, infrageneric classification and historical biogeography of *Mesochila* Rivalier, 1969 (Coleoptera: Cicindelidae), with the performance of different phylogenetic inferences using morphological data compared. Arthropod Systematics & Phylogeny 80: 117–135. https://doi.org/10.3897/asp.80.e76575

Abstract

In this study, we aim to understand the boundaries and the species evolutionary relationships in *Mesochila*, which includes 20 species arranged into three subgenera. We also conducted a biogeographic analysis that allowed us to identify the major events that shaped the currently disjunct distribution of the group. Our analyses were performed employing four major phylogenetic algorithms: equal and implied weight parsimony, maximum likelihood and Bayesian inference. Phylogenetic analyses, including 25 taxa (all 20 species in the genus plus five outgroups) and 37 characters, indicated that *Mesochila* is a monophyletic group composed of four strongly supported lineages, although no consensus was attained regarding relationships between lineages. Bayesian inference resulted in the less resolved topology, whereas implied weight parsimony yielded the most different tree when using a low k value (1). We present a new infrageneric classification for the group with the description of *Mesochila* (*Neomesochila*) **subgen. nov.** to accommodate *M.* (*N.*) *brevipennis*, *M.* (*N.*) *drechseli*, *M.* (*N.*) *moraveci*, and *M.* (*N.*) *prepusula*. Furthermore, we transfer *M.* (*M.*) *distincta* from *M.* (*Eumesochila*) back to *M.* (*Mesochila*). The biogeographical analysis suggested a South American origin for the group, in Chacoan/Paraná dominions (Atlantic rainforest/Cerrado biomes), with subsequent dispersions to Central America and Amazonia.

Key words

morphology, morphological data, Neotropical, new subgenus, Odontocheilina, systematics

1. Introduction

Tiger Beetles (Coleoptera: Cicindelidae) comprise around 2,900 species worldwide (Cassola and Pearson 2000; Wiesner 2020), and are one the most studied Coleoptera groups, resulting in a great deal of knowledge accumulated on their morphology, habits and biology (Pearson 1988; Serrano 2000; Pearson and Vogler 2001; Erwin and Pearson 2008). However, their phylogeny and classification are still elusive, as few studies attempted to resolve phylogenetic relationships within genera (Freitag 1979; Mawdsley 2009, 2011; López-López et al. 2015), subfamilies (Vogler and Pearson 1996; Arndt and Putchkov 1997; Zerm et al. 2007; Gough et al. 2019, 2020; Duran and Gough 2020) or the positioning of this family in Adephaga (López-López and Vogler 2017; Gustafson et al. 2020).

The large Neotropical subtribe Odontocheilina W. Horn, 1899 *sensu* Moravec (2012) was revised recently, with the description of several new species and genera reassessment (summarized by Moravec 2018a, 2020). The former five subgenera of *Pentacomia* Bates, 1940 (Rivalier 1969) were all elevated to a generic status (Moravec and Huber 2015; Moravec 2018a).

Mesochila Rivalier, 1969, which was one of the former subgenera of *Pentacomia*, was originally characterized as possessing traits with a wide range of character states. For instance, body size varies from medium to large; and the labrum may be bicoloured, testaceous or metallic black, green or blue. Additionally, the genus present reduced elytral maculation, and long and slightly sclerotized aedeagus (Rivalier 1969).

The group was subsequently elevated to a generic position, being composed of 20 species, revised and divided into three subgenera (Moravec 2018a, 2020) (Fig.1): *M.* (*Mesochila*), with 13 species, subdivided into two species-groups: *M.* (*M.*) *procera* species-group (five species with a predominant Atlantic rainforest distribution and three distributed in central South America.) and *M.* (*M.*) *smaragdula* species-group (four species in Atlantic Rainforest); *M.* (*Paramesochila*) Moravec, 2018 with three Central American species and one distributed in the northeast Brazil; and *M.* (*Eumesochila*) Moravec, 2018, with two species from central South America, sometimes reaching the Amazonian rainforest, and one species from Atlantic rainforest. So far, most of the Brazilian Amazon, as well as the northeast portion of Brazil, remain without members of the genus, except for *M.* (*P.*) *horni* (Schilder, 1953) and *M.* (*M.*) *moraveci* Roza and Mermudes, 2019. New expeditions and examination of museum collections of those areas may clarify whether this distribution gap is natural or a result of poor sampling.

Although recently revised, *Mesochila* and its subgenera remain hard to diagnose, with several heterogeneous characters. The genus is mainly recognized by a ventral transversal sclerite in the aedeagus, usually referred as ventral spur (Rivalier 1969), which is also variable in shape (Moravec 2018a, 2018b, 2020). The three subgenera are also diagnosed by variable characters, with the following set of characters not varying in the species of each subgenera: *M.* (*Mesochila*) have four toothed mandibles (plus basal molar) and elongate body with notably elongate elytra with parallel to subparallel lateral margins; *M.* (*Eumesochila*) have four toothed mandibles (plus basal molar) and a wider and less oblong shaped elytra; and *M.* (*Paramesochila*) have three toothed mandibles (plus basal molar) and elytra coarsely punctate (Moravec 2018a, 2020).

In this study, we tackled two major problems. Firstly, by conducting the first phylogenetic analysis within the subtribe Odontocheilina, we tested the monophyly and evaluated the boundaries of *Mesochila* and its subgenera, also clarifying its species relationships. Our second goal was to investigate the historical biogeography of *Mesochila* in order to elucidate the major events that shaped the currently disjunct distribution of the group.

2. Material and Methods

2.1. Taxon sampling

To carry out the phylogenetic assessment of the subgenus, a total of 25 species were analysed, which included all currently recognized species of *Mesochila* (20) plus four closely related Odontocheilina species, namely, *Mesacanthina chalceola* (Bates, 1872), *Odontocheila nodicornis* (Dejean, 1825), *Pentacomia speculifera* (Brullé, 1837) and *Phyllodroma lutteomaculata* Chaudoir, 1860. Finally, we used *Opisthencentrus dentipennis* Germar, 1843, to root the tree topology, because this species was never considered congeneric with the remaining species analysed, which all eventually were considered *Odontocheila*.

A total of 424 specimens of 14 South American species of *Mesochila* were examined, including six paratypes of *M. proceroides* Moravec, 2016, housed in the Coleção Entomológica do Instituto Oswaldo Cruz, Rio de Janeiro, Brazil (CEIOC). We also examined 14 specimens referable to the outgroup species. The Central American species of *Mesochila* (*Paramesochila*), *M.* (*Mesochila*) *conformis* (Dejean, 1831), *M.* (*Mesochila*) *drechseli* (Sawada and Wiesner, 1997) and *M.* (*Mesochila*) *prepusula* (Horn, 1907) were not found in the visited collections and thus not examined. However, their character states were possible to obtain from their extensive descriptions and detailed illustrations (Sawada and Wiesner 1997; Duran and Moravec 2013; Moravec and Brzoska 2013; Moravec 2016, 2018a, 2020).

The following institutions lent specimens for this study: CEIOC, Coleção Entomológica do Instituto Oswaldo Cruz, Rio de Janeiro, Brazil; DZRJ, Coleção Entomológica Professor José Alfredo Pinheiro Dutra, Departamento de Zoologia, Universidade Federal do Rio de Janeiro, RJ, Brazil; DZUP, Coleção Entomológica Pe. Jesus Santia-

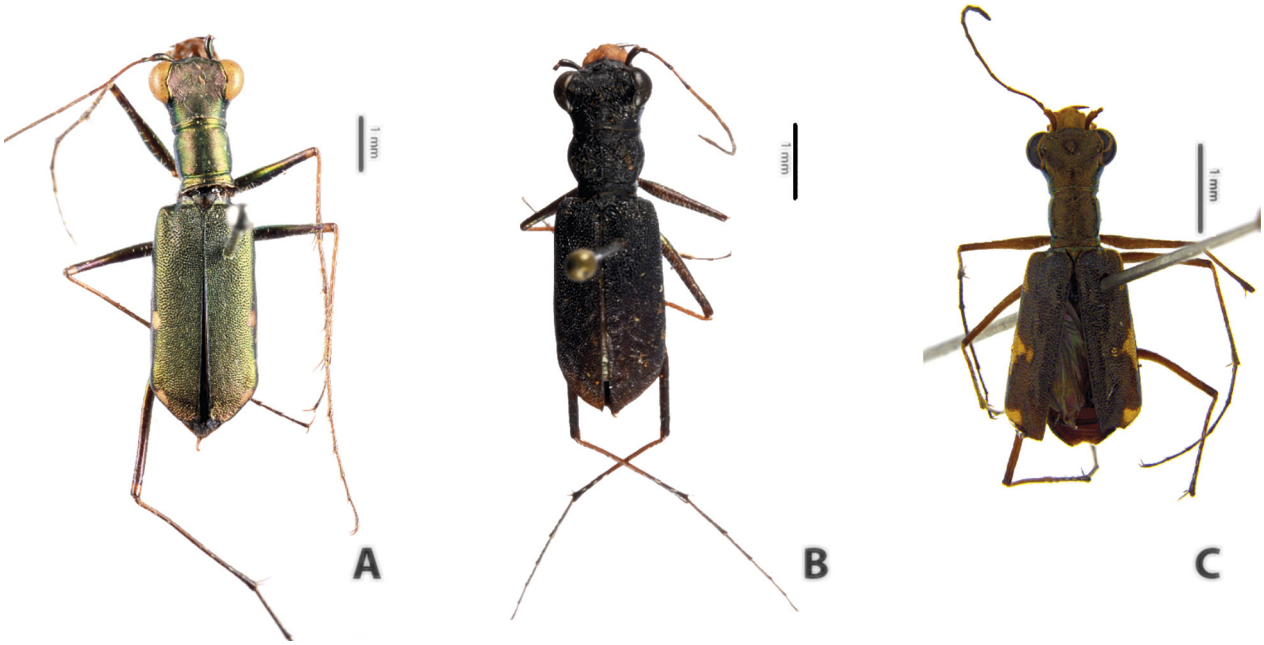

Figure 1. Representatives of *Mesochila* subgenera, *habitus* dorsal: (**A**) *M.* (*Mesochila*) *procera*, (**B**) *M.* (*Eumesochila*) *distigma*, (**C**) *M.* (*Paramesochila*) *horni*.

go Moura, Universidade Federal do Paraná, PR, Brazil; MCNZ, Fundação Zoobotânica do Rio Grande do Sul, RS, Brazil; MNRJ, Museu Nacional, Universidade Federal do Rio de Janeiro, RJ, Brazil; MZSP, Museu de Zoologia, Universidade de São Paulo, SP, Brazil; PUCMG, Pontifícia Universidade Católica de Minas Gerais, MG, Brazil; UNIFEI, Universidade Federal de Itajubá, MG, Brazil.

A complete list of all examined material can be found in the Supporting information, Appendix S1.

2.2. Terminology, dissection and illustrations

The terminology follows Moravec (2018b, 2020). The male genitalia were left in a solution of 10% KOH during 48h in room temperature, in order to clarify the structure and make possible the observation of the sclerites in the inner sac. *Habitus* photographs were made using a Nikon 7000 digital camera with SIGMA 150 mm macrolens. The structures photographs were made on a stereomicroscopy Leica M205C with a coupled digital camera DFC 450 with the Application Suite CV3 montage software. The photographs were edited using Adobe Photoshop and the figure plates were designed with Adobe Illustrator (Adobe Systems).

2.3. Character coding

The coding followed the logical basis presented by Sereno (2007). The matrix was built in MESQUITE v3.2 (Maddison and Maddison 2017), and can be found in the Supporting information, Table S1.

2.4. Phylogenetic analysis

Recently, a debate was brought forth regarding the relative performance of probabilistic phylogenetic methods when dealing with morphological data (Goloboff et al. 2008a; Wright and Hillis 2014; Puttick et al. 2017; Goloboff et al. 2017; O'reilly et al. 2018). The argument lies on the whether Lewis (2001) model, as implemented in both maximum likelihood and Bayesian inference, provides accurate and precise tree topologies when compared to maximum parsimony (Brown et al. 2017; Puttick et al. 2017; Schrago et al. 2018). This prompted us to carry out a comparative evaluation of the performance of the major algorithms in our dataset.

Parsimony analyses were performed with TNT (Goloboff et al. 2008b), under equal (EW) and implied weights (IW) (Goloboff, 1993). All analyses were conducted using heuristic search with branch swapping TBR, employing 10,000 replicates and 100 trees saved for each replicate. For the IW analysis, we explored the topologies obtained under different concavity constant values (k=1, 2, 3, 5, 10, 100). The k values were not chosen with regular intervals because high k values tend to generate uniform and similar results to the ones of EW analysis (Goloboff 2008a). Therefore, analysis with regular k intervals may result in bias toward high k topologies (Mirande 2009). Support was assessed through Symmetric resampling (SR) with 5,000 replicates, because this method is not distorted by implied weights, and absolute Bremer was assessed for EW analysis only (Goloboff et al. 2003).

Character and character states were optimized in WINCLADA, ver. 1.00.08 (Nixon 2002). Following the sensibility analysis criterion (Giribet 2003), we employed the tree topology that was recovered more frequently in our analyses.

Maximum Likelihood (ML) analysis was performed on IQTREE (Nguyen et al. 2015) on its CIBIV Web Server (Trifinopoulos et al. 2016) using ultrafast bootstrap as branch support (Hoang et al. 2018). Bayesian Inference (BI) was performed on MRBAYES 3.2 (Huelsenbeck and Ronquist 2001). The posterior distribution of tree topologies was approximated by the Markov chain Monte Carlo (MCMC) algorithm, which was run for 10,000,000 generations and sampled every 1,000th cycle, with 10% of the initial chains discarded as burn-in. Chain convergence was evaluated in TRACER v1.6 (Rambaut et al. 2014). In both ML and BI, was used the *MKV* model of morphology evolution, modified from *MK* (Lewis 2001). This model implements a Markov process for discrete character evolution accounting for acquisition bias.

2.5. Biogeographic analysis

The geographic distribution of *Mesochila* species and other species on the phylogeny was arranged in five different areas, based on Morrone's dominions (2014a): A (Pacific), B (Boreal Brazilian), C (South Brazilian), D (Chacoan) and E (Paraná). The South-eastern Amazonian dominion had no species recorded. The information about their distribution was based on recent revisions (Pearson et al. 1999; Moravec 2016, 2018; Roza and Mermudes 2017; Moravec 2020). A map was built using QUANTUM-GIS 2.14.3 (QGIS Development Team 2016) with the shapefile of Morrone's dominions (Löwenberg-Neto 2014).

We used S-DIVA (Yu et al. 2010) and Bayesian Binary Method (BBM) (Ronquist and Huelsenbeck 2003) implemented in RASP (Yu et al. 2015) to reconstruct the possible ancestral ranges of *Mesochila* on the phylogenetic trees. To account for phylogenetic uncertainty, we used 20,004 trees from the MCMC output and ran both methods. The BBM was run with the fixed state frequencies model (Jukes-Cantor) with equal among-site rate variation for two million generations, ten chains each, and two parallel runs.

The maximum number of areas in the nodes was set to 5, matching the number of dominions in which the species occurs and allowing for all the possibilities of composed ancestral areas (Kodandaramaiah 2010). The closest outgroup taxa (or clade, if it is the case) was retained in the biogeographical analysis to avoid the bias towards a widespread ancestral in the root (Ronquist 1997; Kodandaramaiah op. cit.).

3. Results

3.1. Newly coded characters for Odontocheilina

We derived 37 characters for investigating *Mesochila* phylogeny, encompassing body size, coloration and external covering, head, thorax, membranous wings and male genitalia. The characters are coded as binary (25) or multistate (12). The characters used in the analysis are as follows (include the length (L), consistent index (CI) and retention index (RI) for the EW analysis):

1. Body Size: (0) 6.0 to 9.3 mm; (1) 9.5 to 14 mm. L = 3; CI = 0.33; RI = 0.81.
2. Head and pronotum, dorsal surface, coloration: (0) green (Fig. 2A); (1) dark green (Fig. 2B); (2) purple (Fig. 2C); (3) black (Fig. 2D); (4) brownish green (Fig. 2E); (5) copper (Fig. 2F). L = 8; CI = 0.62; RI = 0.70.
3. Labrum of the male, relation of width to length: (0) at least 2 times wider than long (Fig. 3G); (1) 1.4 to 1.5 times wider than long (Fig. 3A). L = 4; CI = 0.33; RI = 0.33.
4. Labrum, base coloration in males: (0) green (Fig. 3A); (1) black (Fig. 3B); (2) yellowish brown (Fig. 3C); (3) pale yellow (Fig. 3E). L = 4; CI = 0.75; RI = 0.75.
5. Labrum, base color in females: (0) green; (1) black; (2) yellowish brown; (3) pale yellow. L = 5; CI = 0.60; RI = 0.60.
6. Labrum of the male, median longitudinal macula: (0) absent; (1) present (Fig. 3B). L = 2; CI = 0.50; RI = 0.66.
7. Labrum, margin of laterobasal region, shape: (0) smooth (Fig. 3D); (1) rhomboid (Fig. 3A);(2) long and curved teeth (Fig. 3F); (3) angular (Fig. 3B); (4) short teeth (Fig. 3G). L = 6; CI = 0.66; RI = 0.71.
8. Labrum, lateromedial margin, shape: (0) smooth (Fig. 3J); (1) rhomboid (Fig. 3A); (2) long and curved teeth (Fig. 3F); (3) rounded (Fig. 3D). L = 5; CI = 0.75; RI = 0.66.
9. Labrum, notch before the apical lobe when lateromedial margin is close to apical lobe length: (0) absent; (1) present (Fig. 3E). L = 3; CI = 0.33; RI = 0.60.
10. Labrum, apical lobe, form: (0) smooth or with vestigial teeth (Fig. 3C); (1) two pairs of lateral teeth with a longer medial (Fig. 3J); (2) very long median tooth (Fig. 3H); (3) three long sub-equal teeth (Fig. 3A); (4) a pair of long lateral teeth (Fig. 3F); (5) three short sub-equal teeth (Fig. 3E). L = 5; CI = 1.0; RI = 1.0.
11. Mandible, teeth, quantity: (0) three (Fig. 3K); (1) four (Fig. 3L). L = 1; CI = 1.0; RI = 1.0.
12. Maxillary and labial palpi, coloration: (0) brown, latest article black (Fig. 3M); (1) white, last article black (Fig. 3N); (2) all black (Fig. 3O); (3) all white (Moravec 2020: pl. 71, fig. A). L = 3; CI = 1.0; RI = 1.0.
13. Pronotum, relation of length to width: (0) distinctly wider than long (Fig. 2C); (1) as long as wide (Fig. 2A); (2) distinctly longer than wide (Fig. 2F). L = 6; CI = 0.33; RI = 0.42.
14. Elytra, punctuation: (0) finely punctuated with small and shallow grooves (Fig. 4E); (1) coarsely punctuated with large and deep grooves (Fig. 4F). L = 1; CI = 1.0; RI = 1.0.
15. Elytra, relation of length with width: (0) 3.9–4.2 times longer than wide (Fig. 4A); (1) 3.3–3.6 times longer than wide (Fig. 4D). L = 3; CI = 0.33; RI = 0.81.
16. Elytra, humeral spot, occurrence: (0) absent; (1) present (Fig. 4B). L = 4; CI = 0.25; RI = 0.50.

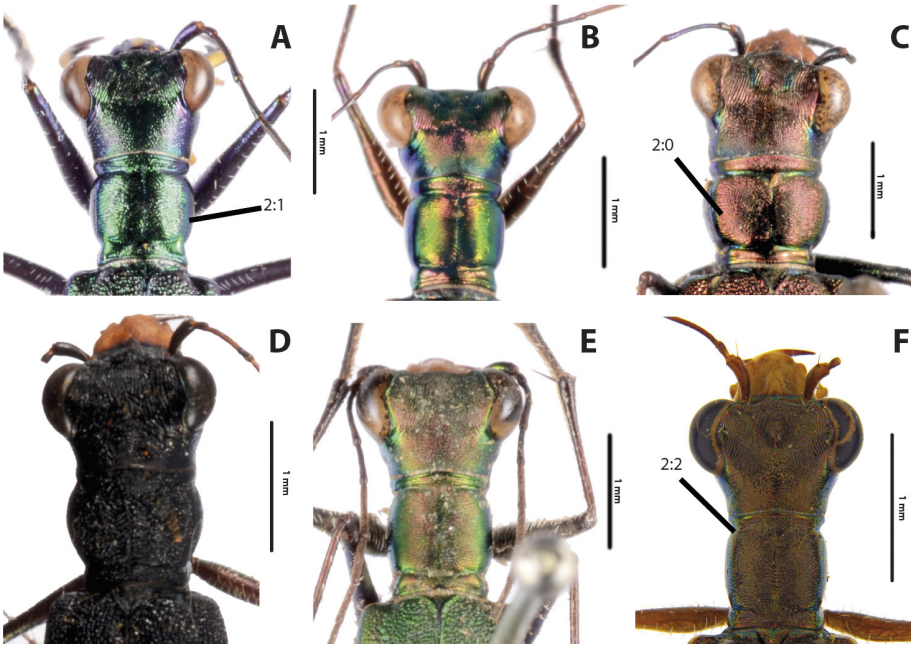

Figure 2. Head and pronotum, dorsal: (**A**) *M.* (*M.*) *biguttata*, (**B**) *M.* (*M.*) *brasiliensis*, (**C**) *M.* (*E.*) *discrepans*, (**D**) *M.* (*E.*) *distigma*, (**E**) *M.* (*M.*) *proceroides*, (**F**) *M.* (*Paramesochila*) *horni*.

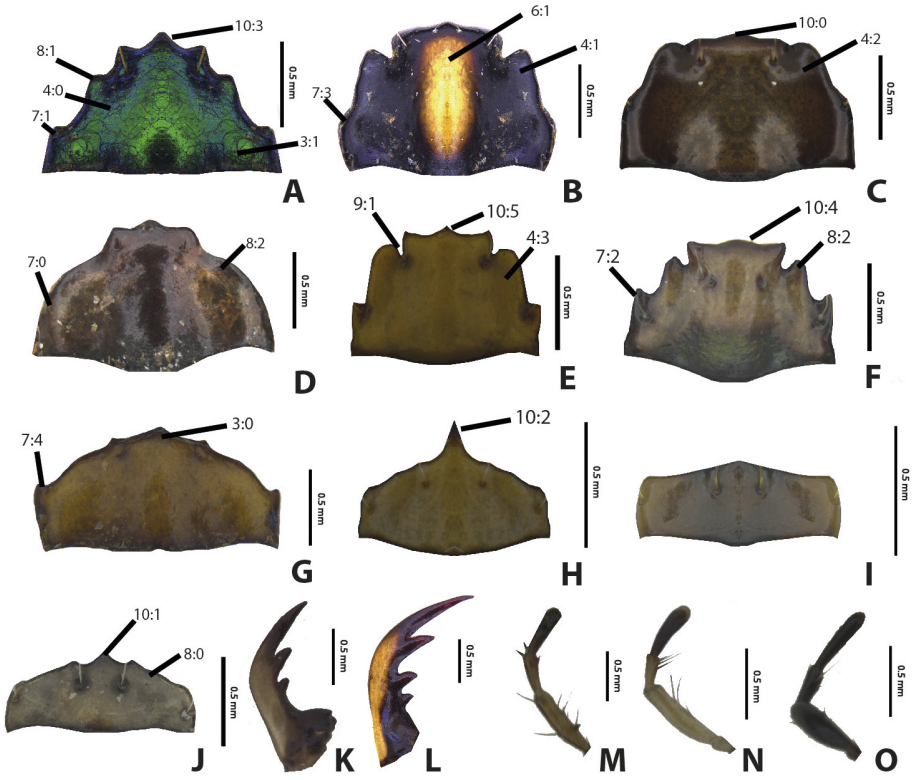

Figure 3. Labrum, male, dorsal: (A) *M.* (*M.*) *cyanneomarginata* (B) *M.* (*M.*) *biguttata* (C) *M.* (*M.*) *brasiliensis* (D) *M.* (*E.*) *distincta* (E) *Pentacomia speculifera* (F) *Odontocheila nodicornis* (G) *M.* (*E.*) *discrepans* (H) *Mesacanthina chalceola* (I). *Opisthencentrus dentipennis* (J) *Phyllodroma lutteomaculata* Mandible, dorsal: (K) *M. (P.) horni* (L) *M.* (*M.*) *smaragdula* mMaxillary palps, dorsal: (M) *M.* (*M.*) *smaragdula.* (N) *Mesacanthina chalceola* (O) *M.* (*M.*) *biguttata*. Numbers marking characters and characters states.

17. Elytra, humeral spot, position: (0) restricted to humerus (Fig. 4H); (1) extending to the end of the basal third of the lateral margin (Fig. 4G). L = 3; CI = 0.33; RI = 0.50.

18. Elytra, lateral and post-middle spot, occurrence: (0) absent; (1) present (Fig. 4A). L = 2; CI = 0.50; RI = 0.0.

19. Elytra, lateral and post-medial spot, shape: (0) subround to subtriangular (Fig. 4A); (1) distinctly triangular (Fig. 4B); (2) rectangular (Fig. 4C); (3) corrugated (Moravec and Brzoska 2014: Fig. 13–15); (4) "half T"-shaped (Fig. 4D). L = 7; CI = 0.57; RI = 0.40.

20. Elytra, latero-apical spot, occurrence: (0) absent; (1) present (Fig. 4B). L = 3; CI = 0.33; RI = 0.50.

21. Elytra, latero-apical spot, dorsal length: (0) reaches approximately half the width of the elytron (Fig. 4C); (1) approximately reaches the elytral suture (Fig. 4D). L = 1; CI = 1.0; RI = 1.0.

22. Membranous wing, radial cell, pigmentation: (0) partial (Fig. 5A); (1) total (Fig. 5B). L = 1; CI = 1.0; RI = 1.0.

23. Membranous wing, cr vein, projection, occurrence: (0) absent (Fig. 5A); (1) present (Fig. 5B). L = 1; CI = 1.0; RI = 1.0.

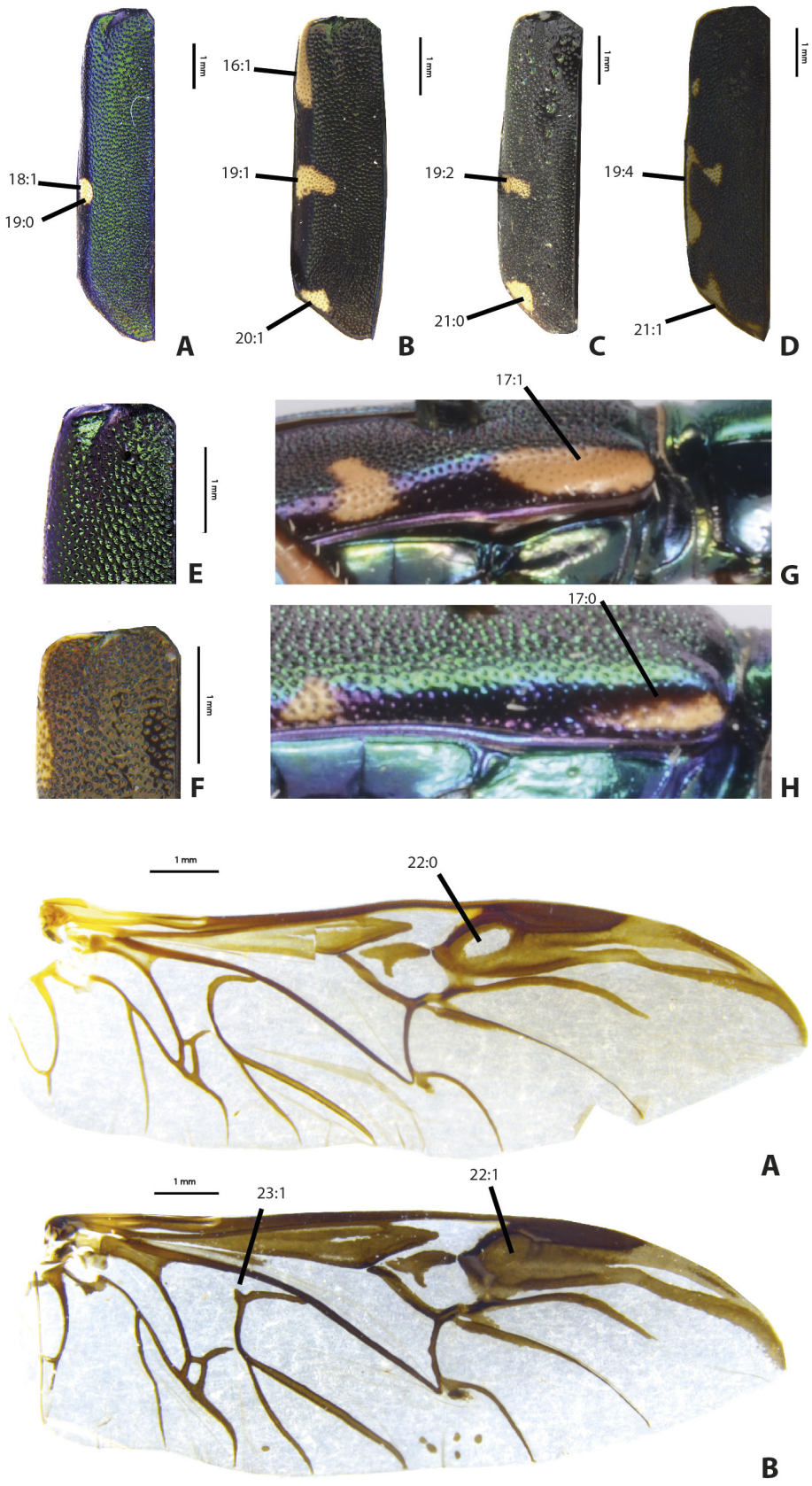

Figure 4. Elytron, dorsal: (**A**) *M.* (*M.*) *biguttata*, (**B**) *M.* (*M.*) *brasiliensis*, (**C**) *M.* (*E.*) *distincta*, (**D**) *Mesacanthina chalceola*. — Elytra, detail of punctuation: (**E**) *M.* (*M.*) *biguttata*, (**F**) *M. (P.) horni.* — Elytron, lateral: (**G**) *M.* (*M.*) *brasiliensis*, (**H**) *M.* (*M.*) *smaragdula*. Numbers marking characters and characters states.

Figure 5. Wing, dorsal: (**A**) *M.* (*M.*) *brasiliensis*, (**B**) *M.* (*M.*) *biguttata*. Numbers marking characters and characters states.

24. Aedeagus, apex, shape: (0) rounded (Fig. 6A); (1) distinctly hook (Fig. 6B); (2) distinctly wide bent rounded beak (Fig. 6C). L = 4; CI = 0.50; RI = 0.78.

25. Aedeagus, apical third, shape: (0) subparallels (Fig. 6C); (1) gradually tapered (6A, 6B); (2) prolonged into narrow, cylindrical and rounded apex (Moravec 2020: pl. 72, figs A–G). L = 3; CI = 0.66; RI = 0.83.

26. Aedeagus, basal part, width: (0) subparallel (Fig. 6A); (1) wide (Moravec 2020: pl. 72, figs A–G). L = 1; CI = 1.0; RI = 1.0.

Figure 6. Aedeagus, lateral view: (**A**) *M.* (*M.*) *biguttata*, (**B**) *M.* (*E.*) *discrepans*, (**C**) *M.* (*M.*) *brevipennis*, (**D**) *Pe. speculifera*, (**E**) *Odontocheila nodicornis.* Numbers marking characters and characters states.

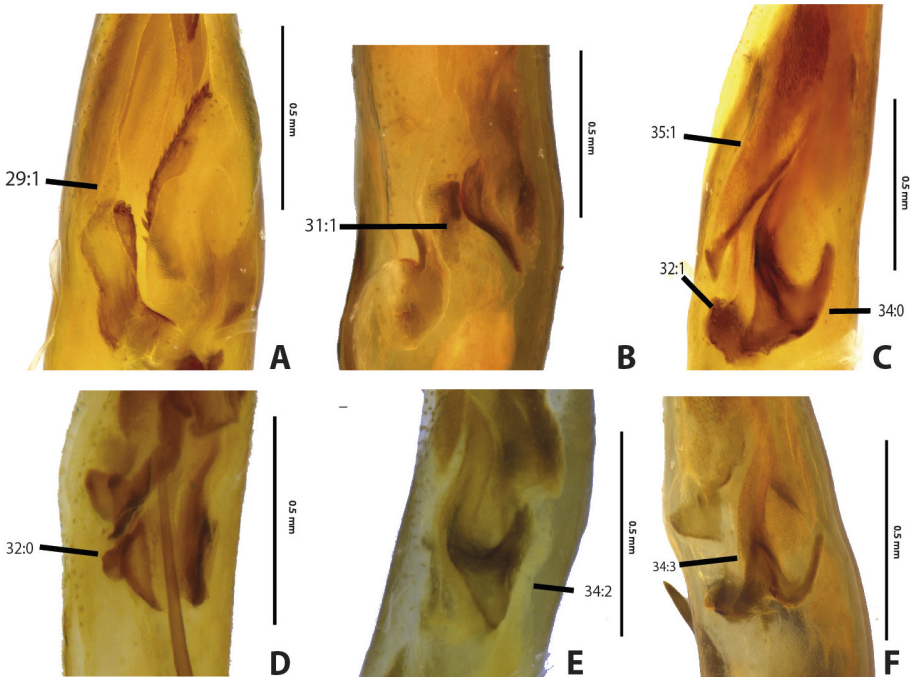

Figure 7. Aedeagus: (**A**) dorsal view, detail of dorsal sclerites of *P.* (*M.*) *biguttata*, (**B**) dorsal view, detail of basal sclerites of *P.* (*M.*) *brasiliensis*, (**C**) lateral view, detail of sclerites of *M.* (*M.*) *smaragdula*, (**D**) lateral view, detail of sclerites of *M.* (*M.*) *brevipennis*, (**E**) lateral view, detail of sclerites of *P.* (*M.*) *distigma*, (**F**) lateral view, detail of sclerites of *P.* (*M.*) *distincta*. Numbers marking characters and characters states.

27. Aedeagus, middle part, width: (0) thin (1/7 of aedeagus length) (Fig. 6B); (1) moderately wide (1/6 of aedeagus length) (Fig. 6A); (2) wide (1/5 of aedeagus length) (Fig. 6E). L = 3; CI = 0.66; RI = 0.89.

28. Aedeagus, sclerites, position inside of aedeagus: (0) apical (Fig. 6D); (1) apical-medial (Fig. 6A); (2) on the entire aedeagus (Fig. 6E). L = 1; CI = 1.0; RI = 1.0.

29. Aedeagus, wavy and spatulate dorsal sclerites, occurrence: (0) absent; (1) present (Fig. 7A). L = 1; CI = 1.0; RI = 1.0.

30. Aedeagus, right dorsal sclerite rod shaped, occurrence: (0) absent; (1) present (Fig. 6B). L = 3; CI = 0.33; RI = 0.33.

31. Aedeagus, proximal sclerites formed by two pieces, occurrence: (0) absent; (1) present (Fig. 7B, 7C). L = 1; CI = 1.0; RI = 1.0.

32. Aedeagus, proximal sclerites form by two pieces, shape: (0) triangular (Fig. 7D); (1) subquadrate (Fig. 7C). L = 2; CI = 0.50; RI = 0.86.

33. Aedeagus, longitudinal ventral sclerite parallel to aedeagus (ventral spur), occurrence: (0) absent; (1) present (Fig. 6A). L = 1; CI = 1.0; RI = 1.0.

34. Aedeagus, longitudinal ventral sclerite parallel to aedeagus, base shape: (0) Stingray-like (Fig. 7C); (1) triangular (Moravec 2020: pl. 72, fig. A–G); (2) bifurcate (Fig. 7E); (3) u-shaped (Fig. 7F). L = 4; CI = 0.75; RI = 0.80.

35. Aedeagus, quadrangular central sclerite with lower sclerotized margin, occurrence: (0) absent; (1) present (Fig. 7C). L = 1; CI = 1.0; RI = 1.0.

36. Aedeagus, quadrangular central sclerite with projected lower left tip, occurrence: (0) absent; (1) present (Fig. 8A). L = 1; CI = 1.0; RI = 1.0.

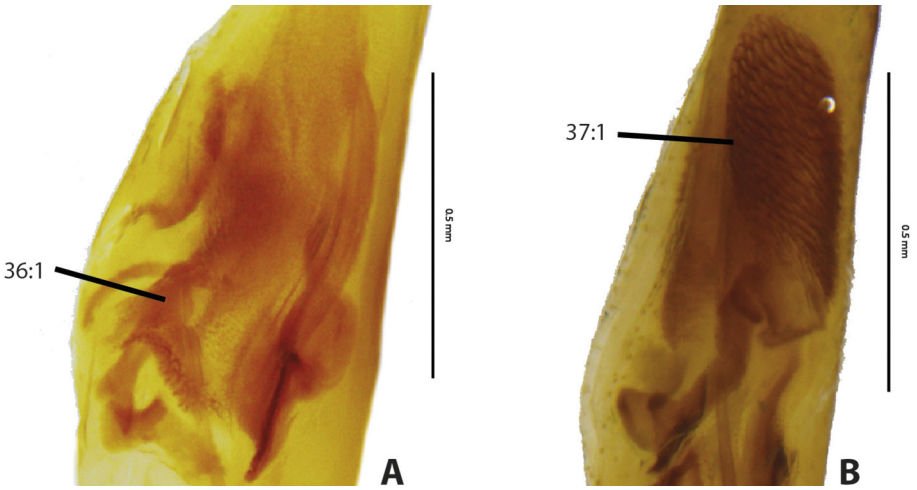

Figure 8. Aedeagus: (**A**) lateral view, detail of sclerites of *M.* (*P.*) *horni*, (**B**) lateral view, detail of central sclerite of *M.* (*M.*) *brevipennis*. Numbers marking characters and characters states.

37. Aedeagus, oval feebly sclerotized central sclerite, occurrence: (0) absent; (1) present (Fig. 8B). L = 1; CI = 1.0; RI = 1.0.

3.2. Phylogenetic analysis

Equally weighted parsimony analysis of the 37 parsimony informative characters resulted in two equally parsimonious trees (L = 106, CI = 0.61, RI = 0.78), both exhibiting identical relationships between *Mesochila* species (Consensus – Fig. 9A, 9B). Implied weights analyses under different concavity constant values (k = 1, 2, 3, 5, 10, 100) yielded exactly the same topology of equally weighted analysis, with the exception of K (1), which recovered a different topology for three ingroup taxa (which will be discussed below).

Mesochila was recovered as monophyletic in all analyses, supported by both Symmetric resampling (64–73) and Bremer (4) supports. The genus is supported by the following synapomorphies: labrum, margin of laterobasal region, shape: angular (7:3, non-homoplastic); aedeagus, sclerites, internal sac positioning: apical-medial (28:1, non-homoplastic); aedeagus, proximal sclerites form by two pieces, occurrence: present (31:1, non-homoplastic); aedeagus, longitudinal ventral sclerite parallel to aedeagus (ventral spur), occurrence: present (33:1, non-homoplastic).

The earliest branching of the *Mesochila* genus separated *Mesochila* (*Paramesochila*) from the remaining species. A subsequent split formed two clades containing *Mesochila* (*Mesochila*) and *Mesochila* (*Eumesochila*) species, which consisted of reciprocally paraphyletic lineages.

The first clade, henceforth referred to as clade A, which contained all species of the subgenus *M.* (*Paramesochila*), was supported by both Symmetric resampling (55–71) and Bremer (3) supports. The synapomorphies for the subgenus were: mandible, teeth, quantity: three (11:0, non-homoplastic); elytra, punctuation, shape: coarsely punctuated with large and deep grooves (14:1, non-homoplastic); aedeagus, quadrangular central sclerite with projected lower left tip, occurrence: present (36:1, non-homoplastic). *Mesochila* (*P.*) *horni* Schilder, 1953 was found as sister to all other *M.* (*Paramesochila*) species.

The phylogenetic relationships of the remaining species – *M.* (*P.*) *wappesi* (Moravec and Brzoska, 2013), *M.* (*P.*) *skrabali* (Duran and Moravec, 2013) and *M.* (*P.*) *tayutica* Moravec, 2018 – were recovered as a polytomy in all analyses. The evolutionary affinity of these three species was the better-supported within the genus, with high values of both Symmetric Resampling (99) and Bremer (12) supports. The synapomorphies of the Central American species were: head and pronotum, dorsal surface, coloration: dark green (2:1, non-homoplastic); maxillary and labial palpi, coloration: all white (12:3, non-homoplastic); elytra, humeral spot, position: (0) restricted to humerus (17:0, homoplastic); elytra, latero-apical spot, dorsal length: approximately reaches the elytral suture (21:1, non-homoplastic); aedeagus, apical third, shape: prolonged into narrow, cylindrical and rounded apex (25:2, homoplastic); aedeagus, basal part, width: wide (26:1, non-homoplastic); aedeagus, middle part, width: wide (27:2, homoplastic); aedeagus, right dorsal sclerite rod shaped, occurrence: present (30:1, homoplastic); aedeagus, longitudinal ventral sclerite parallel to aedeagus, base shape: triangular (35:1, non-homoplastic).

A second clade, named clade B, was formed by *M.* (*Mesochila*) and *M.* (*Eumesochila*) species, although with low support values. It was characterized by a single synapomorphy: aedeagus, apex, shape: thin hook (24:1, non-homoplastic). Clade B was divided into two subclades: clade C, composed of *M.* (*E.*) *distigma* (Dejean, 1825) + *M.* (*E.*) *discrepans* (Horn, 1893) as sister group to *M.* (*M.*) *drechseli* (Sawada and Wiesner, 1997) + a polytomy containing *M.* (*M.*) *brevipennis* (W. Horn, 1907), *M.* (*M.*) *prepusula* (W. Horn, 1907) and *M.* (*M.*) *moraveci* Roza and Mermudes, 2019; and the other (Clade D) composed of the remaining species of the genus.

The clade C has low support values with two synapomorphies: elytra, humeral spot, occurrence: absent (16:0, homoplastic); aedeagus, middle part, width: thin (27:0, non-homoplastic). The clade *M.* (*E.*) *distigma* + *M.* (*E.*) *discrepans* was supported by both Symmetric resampling (50–65), at least in most analyses, and Bremer (3) sup-

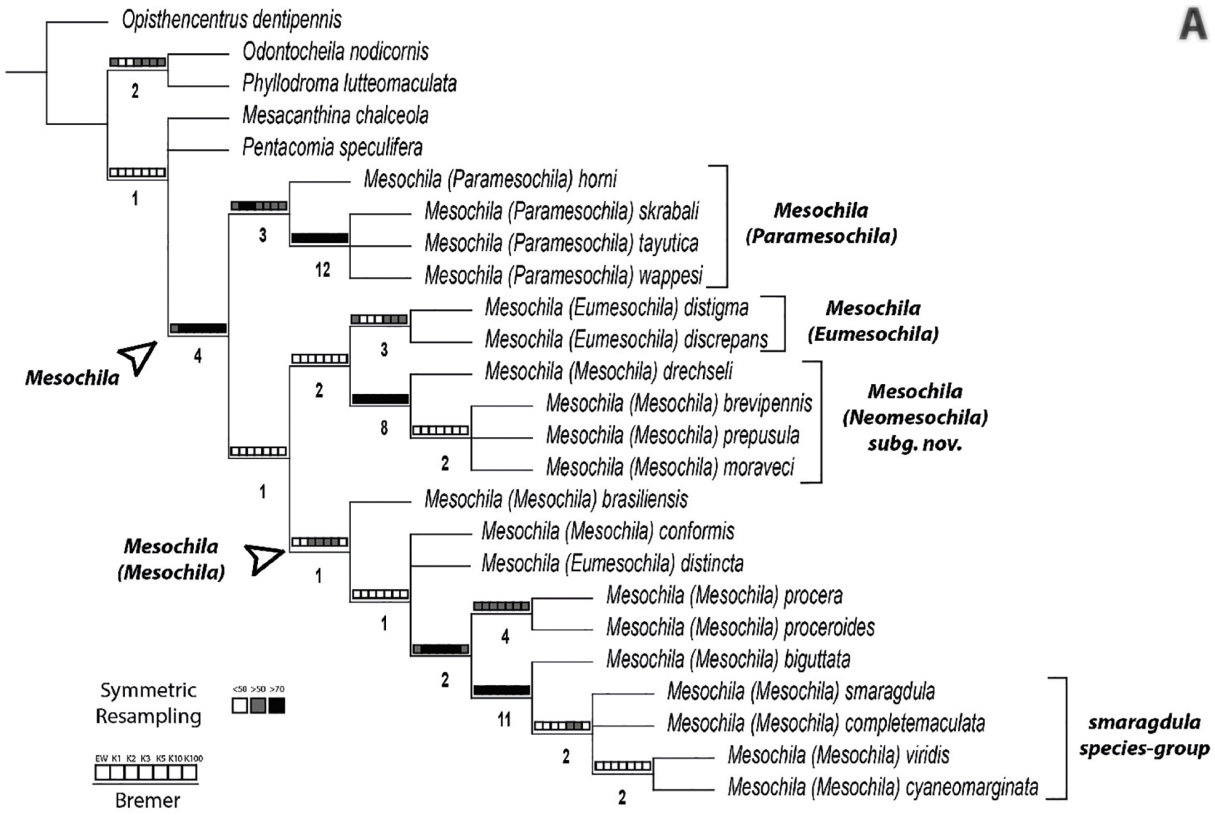

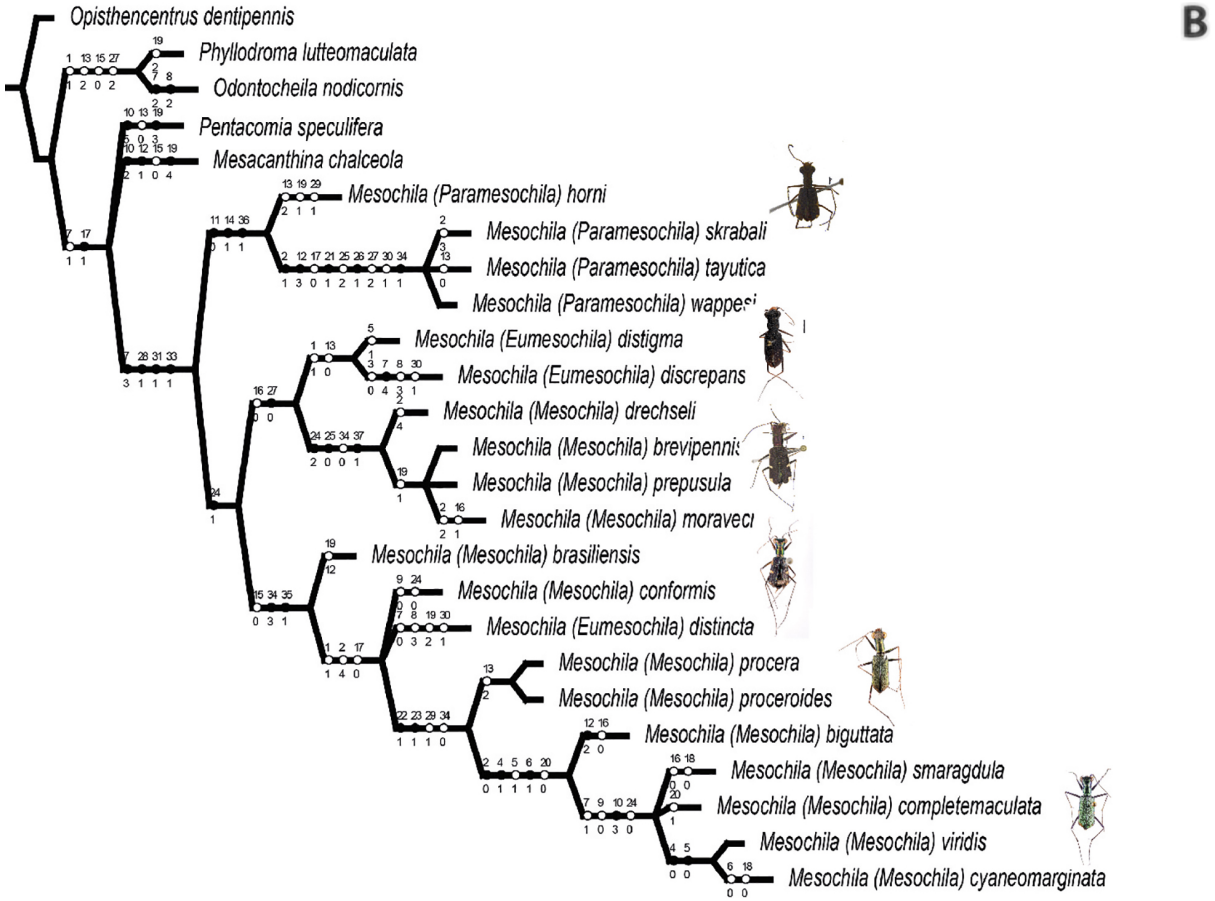

Figure 9. Phylogenetic relationship of *Mesochila*: (**A**) Consensus tree found on the EW and IW (Except K=1) parsimony analysis. Above the branches are marked the Symmetric Resampling, and bellow the Bremer supports. More legends in the figure. (**B**) Phylogenetic relationship of *Mesochila* found on the EW and IW (Except K=1) parsimony analysis. Non-homoplastic synapomorphies are marked with black spots, while homoplastic ones are marked with white spots.

port. The clade was sustained by two synapomorphies: body size: 9.5 to 14 mm (1:1, homoplastic); pronotum, relation of length to width: distinctly wider than long (13:0, homoplastic). Its sister clade, *M.* (*M.*) *drechseli* + a polytomy of *M.* (*M.*) *brevipennis*, *M.* (*M.*) *prepusula* and *M.* (*M.*) *moraveci* (herein designed as *brevipennis* species-group) is supported by both Symmetric Resampling (80–89) and Bremer (8) supports, and presents the following synapomorphies: aedeagus, apex, shape: distinctly wide bent rounded beak (24:2, non-homoplastic); aedeagus, apical third, shape: subparallels (25:0, non-homoplastic); aedeagus, longitudinal ventral sclerite parallel to aedeagus, base shape: stingray-like (34:0, homoplastic); aedeagus, oval feebly sclerotized central sclerite, occurrence: present (37:1, non-homoplastic). The polytomy implicate *M.* (*M.*) *brevipennis*, *M.* (*M.*) *prepusula* and *M.* (*M.*) *moraveci* has low support values, and only one synapomorphy: elytra, lateral and post-medial spot, shape: distinctly triangular (19:1, homoplastic).

The clade D had low Bremer support and Symmetric Resampling values of above 50 only in two IW analyses. The group has three synapomorphies: elytra, relation of length with width: 3.9–4.2 times longer than wide (15:0, homoplastic); aedeagus, longitudinal ventral sclerite parallel to aedeagus, base shape: u-shaped (34:3, non-homoplastic); aedeagus, quadrangular central sclerite with lower sclerotized margin, occurrence: present (35:1, non-homoplastic). *M.* (*M.*) *brasiliensis* (Dejean, 1825) was found as the sister group of the rest of the species. Next, a polytomy of *M.* (*M.*) *conformis* (Dejean, 1831) and *M.* (*E.*) *distincta* (Dejean, 1831) was recovered as the sister group to the rest of Clade D. This topology has low support value in all analyses for both supports and has only three synapomorphies: body size: 9.5 to 14 mm (1:1, homoplastic); head and pronotum, dorsal surface, coloration: brownish green (2:4, homoplastic); elytra, humeral spot, position: restricted to humerus (17:0, homoplastic).

The only different tree recovered a clade formed by (M. (M.) conformis + (M. (M.) brasiliensis + M. (E.) distincta)) as sister to the rest of clade D in the K1 analysis. This topology, however, presented low support value.

Next, the lade E formed by *M.* (*M.*) *procera* (Chaudoir, 1860) and *M.* (*M.*) *proceroides* Moravec, 2016 recovered as sister of *M.* (*M.*) *biguttata* (Dejean, 1825) and all the *smaragdula* species-group *sensu* Moravec (2020). This position is supported by Symmetrical Resampling (60–74) and Bremer (2) supports. They share the following synapomorphies: membranous wing, radial cell, pigmentation: total (22:1, non-homoplastic); membranous wing, cr vein, projection, occurrence: present (23:1, non-homoplastic); aedeagus, wavy and spatulated dorsal sclerites, occurrence: present (29:1, homoplastic); aedeagus, longitudinal ventral sclerite parallel to aedeagus, base shape: Stingray-like (34:0, homoplastic). The clade *M.* (*M.*) *procera* + *M.* (*M.*) *proceroides* was well supported by Symmetrical resampling (63–65) and Bremer (4) supports, but shares only one synapomorphy: pronotum, relation of length to width: distinctly longer than wide (13:2, homoplastic).

The clade formed by *M.* (*M.*) *biguttata* and all the *smaragdula* species-group was highly supported by Symmetrical Resampling (83–86) and Bremer (11) supports, and share five synapomorphies: head and pronotum, dorsal surface, coloration: green (2:0, non-homoplastic); labrum, base coloration in males: black (4:1, non-homoplastic); labrum, base color in females: black (5:1, homoplastic); labrum, median longitudinal macula in the male, occurrence: present (6:1, non-homoplastic); elytra, latero-apical spot, occurrence: absent (20:0, homoplastic).

Inside *smaragdula* species-group, it was found a polytomy of *M.* (*M.*) *smaragdula* (Dejean, 1825), *M.* (*M.*) *completemaculata* (Horn, 1922) and a clade formed by *M.* (*M.*) *viridis* (Dejean, 1831) and *M.* (*M.*) *cyaneomarginata* (Horn, 1920). It is supported by Bremer (2) support, but has low support from Symmetrical Resampling, except in K10 and K100 analyses (51). Presents four synapomorphies: labrum, margin of laterobasal region, shape: (1) rhomboid (7:1, homoplastic); labrum, notch before the apical lobe when lateromedial margin is close to apical lobe length, occurrence: absent (9:0, homoplastic); labrum, apical lobe, form: three long sub-equal teeth (10:3, non-homoplastic); aedeagus, apex, shape: rounded (24:0, homoplastic). The clade formed by *M.* (*M.*) *viridis* and *M.* (*M.*) *cyaneomarginata* is supported by Bremer support (2) but has low values of Symmetrical resampling in all analyses. It shares two synapomorphies: labrum, base coloration in males: green (4:0); labrum, base coloration in females: green (5:0).

ML analysis recovered a tree with log-likelihood score of -ln 471.111 (Fig. 10A), with topological relationships very similar to that of maximum parsimony. *Mesochila* was also recovered as monophyletic, with high support of Ultrafast bootstrap (95). The main differences between ML and MP trees concerned the resolution of the polytomies recovered by MP. The ML-resolved groups consisted of: (*M.* (*P.*) *tayutica* + (*M.* (*P.*) *wappesi* + *M.* (*P.*) *skrabali*)) in clade A, (*M.* (*M.*) *moraveci* + (*M.* (*M.*) *drechseli* + (*M.* (*M.*) *brevipennis* + *M.* (*M.*) *prepusula*))) in clade C, (*M.* (*M.*) *brasiliensis* + (*M.* (*E.*) *distincta* + (*M.* (*M.*) *conformis* + rest of clade D))) in clade D, and (*M.* (*M.*) *smaragdula* + (*M.* (*M.*) *completemaculata* + (*M.* (*M.*) *viridis* + *M.* (*M.*) *cyaneomarginata*))) in *smaragdula* species group. However, most of these groups were poorly supported by ultrafast bootstrap values below 95 (Minh et al. 2013). The exceptions were clade A, the Central American species clade, Clade E and *M.* (*M.*) *biguttata* + *smaragdula* species group clade.

BI also recovered a tree topology (Fig. 10B) similar to the MP tree, but the occurrence of polytomies was higher. Apart from *Mesochila*, which was consistently monophyletic with a high posterior clade probability (PP = 0.99), the Central American species clade, *M.* (*M.*) *brevipennis* clade, clade E and *M.* (*M.*) *biguttata* + *smaragdula* species group clade (all with PP > 95), the statistical support for clades in the Bayesian tree was overall low. BI–MP differences were as follows: clade A was recovered in a polytomy with clade C and clade D; The Central American species were also recovered as a polytomy; *M.* (*M.*)

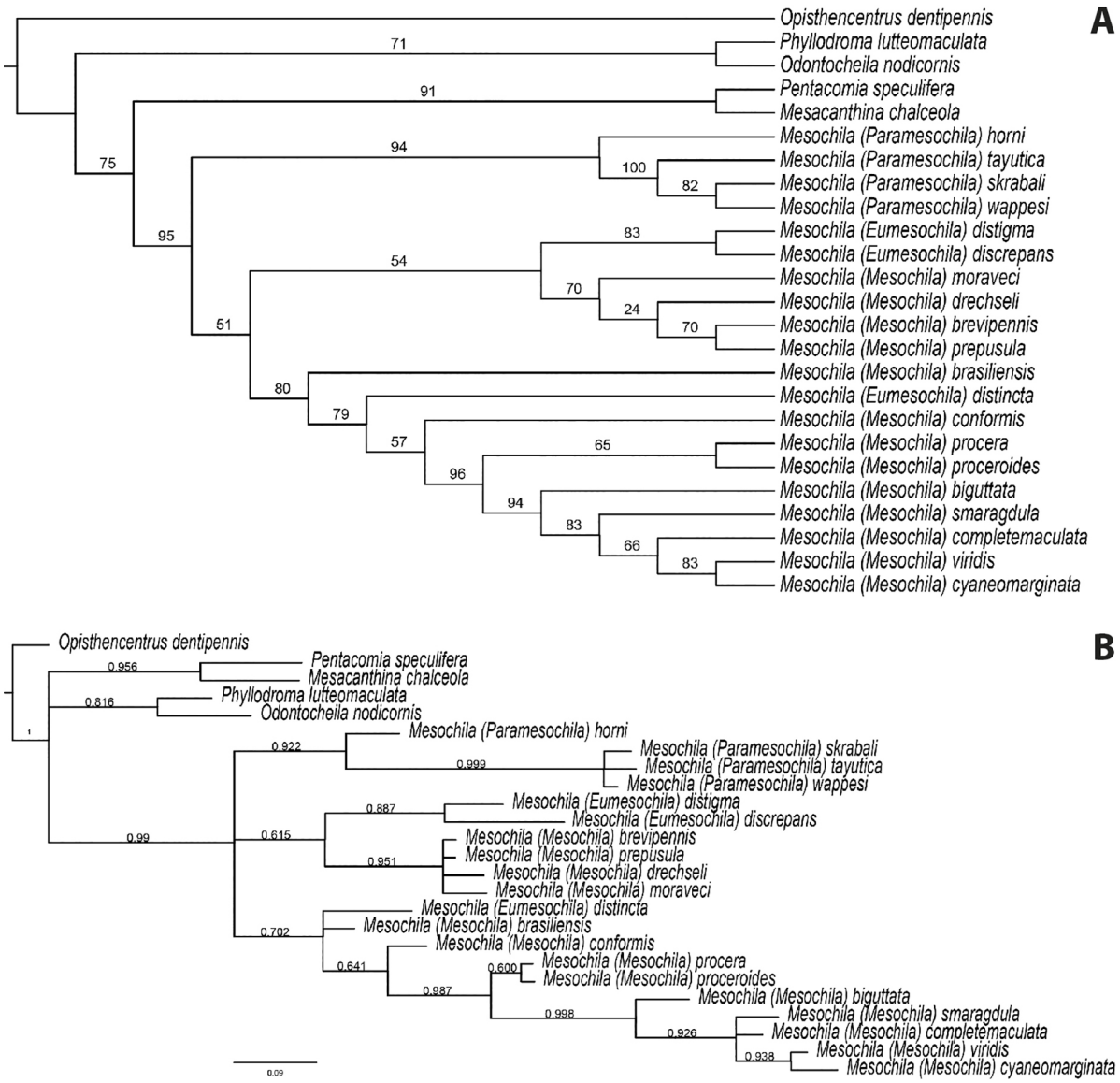

Figure 10. Phylogenetic relationship of *Mesochila*: (**A**) Phylogeny found on the ML analysis, with a likelihood score of -ln 471.111. Above the branches is marked the Ultrafast *bootstrap* score. (**B**) Phylogenetic relationship of *Mesochila* found on the Bayesian analysis. Above the branches is marked the posterior probability.

brevipennis clade was also found as a polytomy; *M.* (*M.*) *brasiliensis* and *M.* (*E.*) *distincta* were found in a polytomy at the base of clade D.

3.3. Biogeographic analysis

The map of the distribution (Fig. 11) showed that most species are restrained to one or two dominions, with the exception of *M.* (*E.*) *discrepans* and *M.* (*E.*) *distigma*. Both these species are widely amplilocated. We performed the S-DIVA and BMM analyses for the topology yielded by the ML analysis (Fig. 12, 13), since both methods require a polytomy-free tree topology as input. Because topological variation between phylogenetic methods was not significant, and the ML-resolved polytomies concerned mainly lineages with the same dominion distribution, we expect that the adoption of a fully resolved tree had little impact in the biogeographic analysis.

The S-DIVA analysis inferred 18 dispersal and three vicariant events (Fig. 12). The most likely ancestral area of *Mesochila* (node 42) was recovered as area E with 51% marginal probability. Other possibilities were area D (29% probability) and area DE (18% probability). The analysis estimated a 5% probability of two dispersion events from this original area E to areas E and EAD separately. The ancestral distribution of the clade A (node 26) was assigned to ADE (35% probability), AE (34%) or AD (31%). There is 34% probability of a vicariant event from area ADE to area A and DE, and A is the ancestral area of the Central American species (node 25) with 100% probability. The following node on the Central American clade (node 24) has ancestral area A (100% probability) with no dispersal or vicariant events.

The ancestral area of the clade B (node 41) was recovered as E (35% probability), followed by DE (33%) or D (31%). The analysis recovered a 9% chance of one vicariant event separating area DE into areas D and E.

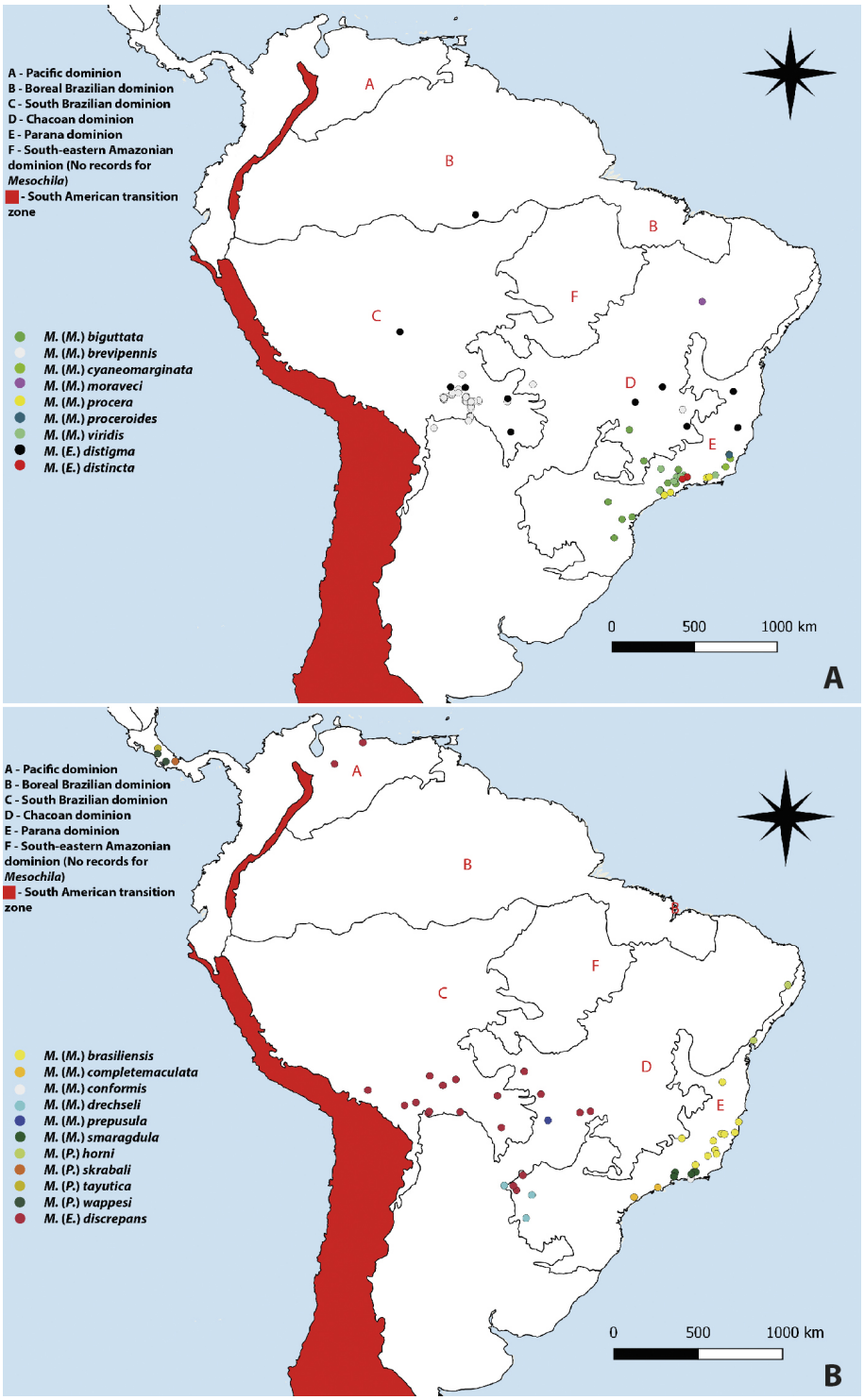

Figure 11. Distribution of *Mesochila* species: (**A**) *M.* (*M.*) *biguttata*, *M.* (*M.*) *brevipennis*, *M.* (*M.*) *cyaneomarginata*, *M.* (*M.*) *moraveci*, *M.* (*M.*) *procera*, *M.* (*M.*) *proceroides*, *M.* (*M.*) *viridis*, *M.* (*E.*) *distigma*, *M.* (*E.*) *distincta*. (**B**) Distribution of *M.* (*M.*) *brasiliensis*, *M.* (*M.*) *completemaculata, M.* (*M.*) *conformis, M.* (*M.*) *drechseli*, *M.* (*M.*) *prepusula*, *M.* (*M.*) *smaragdula*, *M.* (*P.*) *horni*, *M.* (*P.*) *skrabali*, *M.* (*P.*) *wappesi*, *M.* (*P.*) *tayutica, M.* (*E.*) *discrepans*. Letters representing following areas: A (Pacific), B (Boreal Brazilian), C (South Brazilian), D (Chacoan), E (Paraná) and F (South-eastern Amazonian).

Clade C (node 31) has the ancestral D (41% probability) or DE (36%), with alternative areas E (18%), with 15% chance of one dispersal event, D to DE, and one vicariant event separating area DE into area D and E. Inside Clade C, *M.* (*E.*) *distigma* + *M.* (*E.*) *discrepans* clade (node 27) has the ancestral area of E (50% probability) or D (49%). There is 50% probability of six dispersal events, which rendered the current amplilocate distribution of *M.* (*E.*) *distigma* and *M.* (*E.*) *discrepans*. In the other clade, *brevipennis* species-group (node 30) had the ancestral area D (73% probability), or alternatively DE (27%). The subsequent ancestral areas of the group were also most likely D (100% probability). There is one dispersion in node 29 (for *M. drechseli* – DE) and other in node 28 (for *M. brevipennis* – CD).

The clade D has the ancestral area (node 40) of E (66% probability), or alternatively DE (33%). There is 70% possibility of one dispersal event from area E to area DE. All subsequent nodes have most likely the ancestral area of E (100% probability), with dispersal events happening on node 36 (100% chance for *M. biguttata* – DE).

The BMM analysis resulted in the possibility of 22 dispersal and one vicariance events (Fig. 13). The most likely ancestral area of *Mesochila* (node 42) was recov-

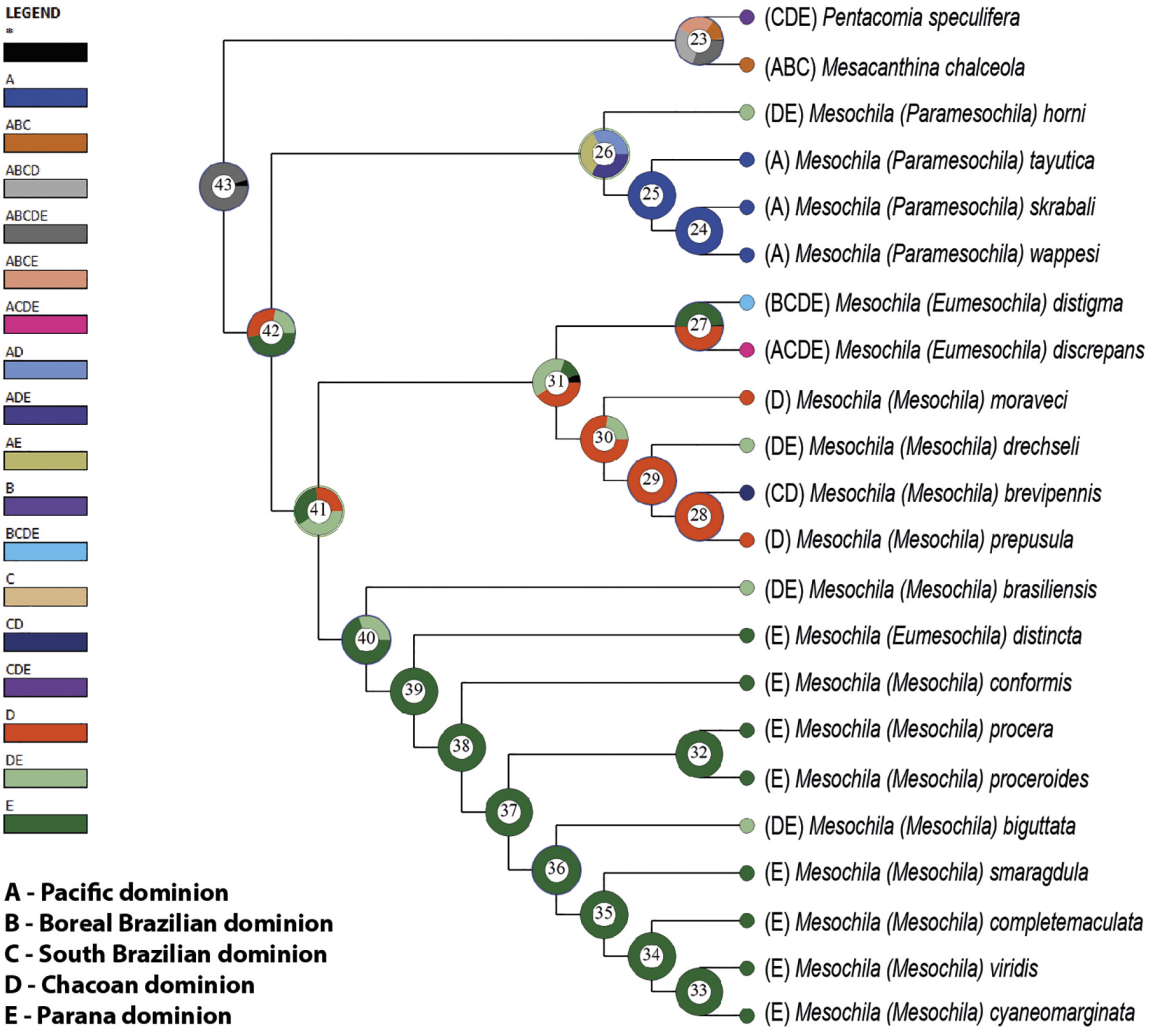

Figure 12. Ancestral area reconstruction by S-DIVA analysis: Letters representing following areas: A (Pacific), B (Boreal Brazilian), C (South Brazilian), D (South-eastern Amazonian), E (Chacoan) and F (Paraná).

ered as a composed area of two different areas (DE) with 69% marginal probability. Other possibilities were area D (17% probability) and area E (8% probability). There are 32% probability of two events of dispersion from this original DE area to areas D and E separately, and posterior colonization of area DE independently in the two following ancestral nodes. The ancestral distribution of the clade A (node 26) was found as most probable as area DE (with 57% probability), and alternative areas being D (27%) or E (10%). There is 50% probability of a dispersal to area DEA, with a subsequent vicariant event separating area A, which is ancestral area of the Central American species (node 25) with 88% probability (alternative area AD presented 6% probability). The following node on the Central American clade (node 24) has ancestral area A (99% probability) with no dispersal or vicariant events.

The ancestral area of the clade B (node 41) was recovered as DE (81% probability), with alternative area D (8%) or CDE (6%). There is 39% chance of two dispersal events in similar way of node 42. Clade C (node 31) has the ancestral DE (55% probability), with alternative areas CDE (26%) and D (10%). There is 18% chance of two dispersal events, one from are DE to area D, and other from are DE to area CDE. Inside Clade C, *M.* (*E.*) *distigma* + *M.* (*E.*) *discrepans* clade (node 27) has the ancestral area of CDE (63% probability), with two alternative ancestral areas: BCDE (17%) and ACDE (8%). There is 62% probability of five dispersal events, which rendered the current amplilocate distribution of *M.* (*E.*) *distigma* and *M.* (*E.*) *discrepans*. In the other clade, b*revipennis* species-group (node 30) had the ancestral area D (53% probability), or alternatively DE (35%) or CD (7%). The subsequent ancestral areas of the group were also most likely D. There is one dispersion in node 29 (for *M. drechseli* – DE) and other in node 28 (for *M. brevipennis* – CD).

Clade D has the ancestral area (node 40) of DE (87% probability), or alternatively E (10%). There is 77% possibility of one dispersal event from area DE to area E. All subsequent nodes have most likely the ancestral area of E (at least 70% probability), with dispersal events happening on node 36 (67% chance for *M. biguttata* – DE).

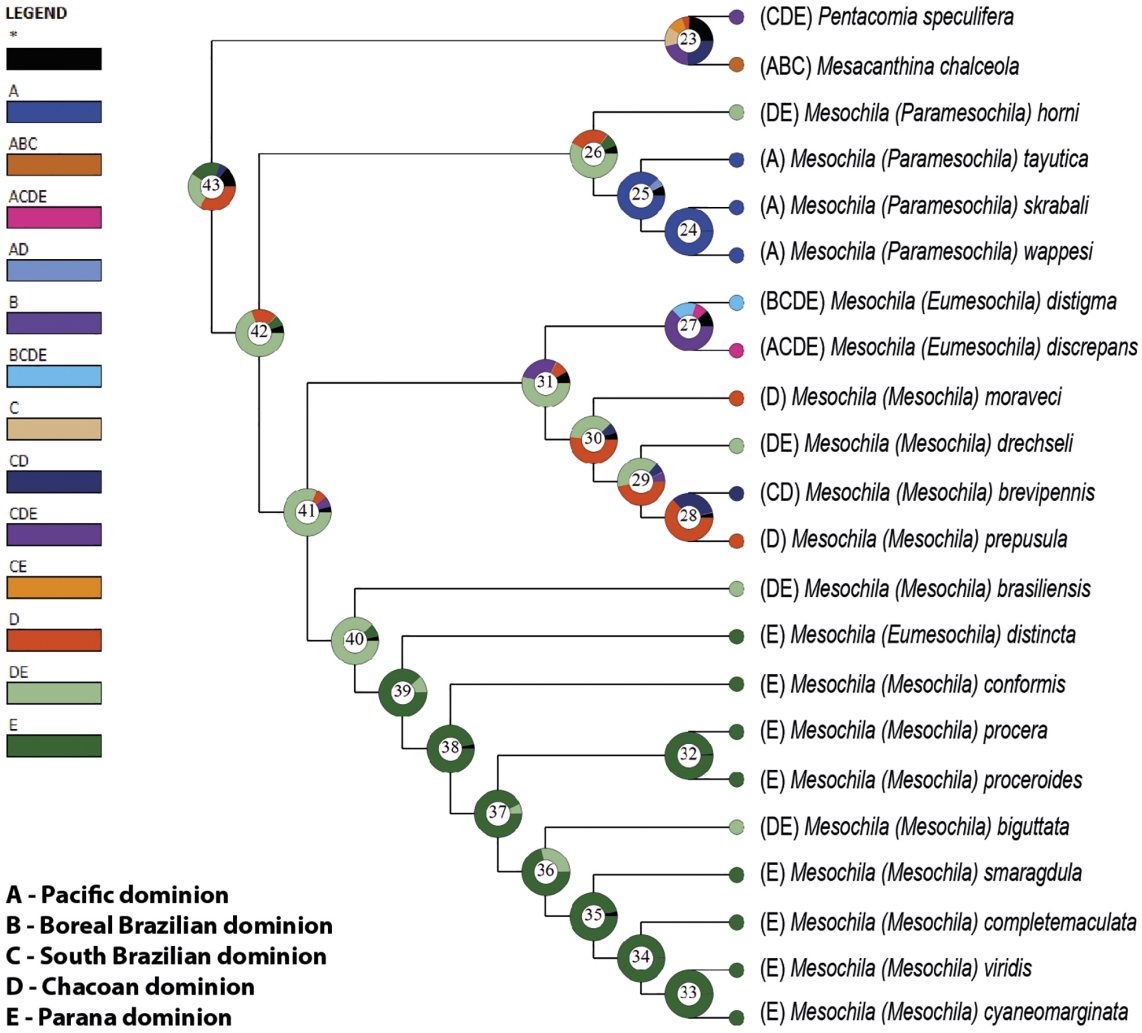

Figure 13. Ancestral area reconstruction by BMM analysis: Letters representing following areas: A (Pacific), B (Boreal Brazilian), C (South Brazilian), D (South-eastern Amazonian), E (Chacoan) and F (Paraná).

4. Discussion

4.1. Phylogenetic analysis

Here we presented the first phylogeny of an Odontocheilina lineage. Tree topologies obtained by MP and ML were well resolved, with the exception of two internal clades, in clade A and C, and four taxa inside clade D. BI yielded considerably more polytomies, including the earliest branching of *Mesochila*. Overall, homoplasy likely had little impact on the results, since the topology found by the implied weight analysis was identical to the equal weight parsimony analysis. Although most analyses generated groups with low support values, the main clades inside *Mesochila* (clade A, *M.* (*E.*) *discrepans* + *M.* (*E.*) *distigma* clade, *brevipennis* species-group and clade D) were usually well supported. Besides that, topologies were consistent across different analyses, which corroborates employing this phylogeny to evaluate the systematics of this group.

The topologies generated by MP and ML exhibited better resolutions when compared with the Bayesian tree. In theory, previous studies have reported that BI of morphological data is accurate, meaning the true tree frequently lies within the 95% credibility interval of topologies. However, higher accuracy generally comes at the expense of lower precision, resulting in trees with lower resolution, especially in small datasets, as the present study (O'reilly et al. 2016; Puttick et al. 2017; Schrago et al. 2018). This prompted some authors to advocate in favour of the implied weight analysis for morphological characters (Goloboff et al. 2017). The debate around this subject is ongoing and generally there is a lack of studies employing empirical analyses instead of simulations. The only exception is the recent study of Schrago et al. (2018), who carried out an extensive comparative evaluation of MP and BI using more than 100 published matrices from MorphoBank. The authors confirmed the results from simulations, showing that BI under the MKv model generates wide credibility intervals and, consequently, lower resolution.

Based on the present study, *Mesochila* is a well-supported monophyletic group, including all 20 species previously assigned to the genera. We obtained, however, a different configuration for the subgenera. *M.* (*Parame-*

sochila) was recovered as a well-supported phylogenetic group, with *M.* (*P.*) *horni* as sister group to the remaining species. The other subgenera, *M.* (*Mesochila*) and *M.* (*Eumesochila*) were recovered as reciprocally paraphyletic.

We identified three main clades, in clade B, which were recovered in all analyses, usually well-supported: *M.* (*E.*) *discrepans* + *M.* (*E.*) *distigma* (which corresponds with *M.* (*Eumesochila*) with the exclusion of *M.* (*E.*) *distincta*; *brevipennis* species-group, which was placed outside of the main *M.* (*Mesochila*) clade; and clade C, which includes the remaining *M.* (*Mesochila*) species with the inclusion of *M.* (*E.*) *distincta*. The position of three taxa at clade C, *M.* (*M.*) *brasiliensis*, *M.* (*M.*) *conformis* and *M.* (*E.*) *distincta*, is weakly supported and varied between analyses. Their morphological resemblance with the rest of clade D, however, makes their inclusion in this group more likely. Due to the fact that this four previous mentioned clades were stable in all analyses carried out, frequently highly supported, we were prompted to propose a new infrageneric configuration for the genus:

Genus *Mesochila* Rivalier

Type species. *Odontocheila procera* Chaudoir, 1860 (by original designation)

Mesochila (*Paramesochila*) Moravec

Type species. *Pentacomia* (*Mesochila*) *skrabali* Duran and Moravec, 2013

Diagnosis. Smaller body length, usually between 6–9.3 mm; mandibles with only three teeth (plus molar one); pronotum usually as wide as long; elytra 3.3–3.6 times longer than wide, coarsely punctate; aedeagus shape variable, usually very wide, and internal sac shape variable.

4 species included:
- *M.* (*P.*) *horni* (Schilder, 1953)
- *M.* (*P.*) *skrabali* (Duran and Moravec, 2013)
- *M.* (*P.*) *wappesi* (Moravec and Brzoska, 2013)
- *M.* (*P.*) *tayutica* Moravec, 2018

Mesochila (*Eumesochila*) Moravec

Type species. *Cicindela distigma* Dejean, 1825 (by original designation)

Diagnosis. Larger body length, usually between 9.5–14 mm; mandibles with four teeth (plus molar one); pronotum distinctively wider than long. elytra 3.3–3.6 times longer than wide, finely punctate; aedeagus very thin and distinctly hooked, internal sac sclerites shape variable.

2 species included:
- *M.* (*E.*) *discrepans* (W. Horn, 1893)
- *M.* (*E.*) *distigma* (Dejean, 1825)

Mesochila (*Mesochila*) Rivalier

Type species. *Odontocheila procera* Chaudoir, 1860 (by original designation)

Diagnosis. Larger body length, usually between 9.5–14 mm; mandibles with four teeth (plus molar one); pronotum usually as wide as long, sometimes longer than wide; elytra 3.9–4.2 times longer than wide, finely punctuate; aedeagus internal sac with stingray-like or u-shaped ventral spur and quadrangular central sclerite with lower sclerotized margin.

10 species included:
M. (*M.*) *biguttata* (Dejean, 1825)
M. (*M.*) *brasiliensis* (Dejean, 1825)
M. (*M.*) *completemaculata* (W. Horn, 1922)
M. (M.) cyaneomarginata (W. Horn, 1900)
M. (*M.*) *conformis* (Dejean, 1831)
M. (*M.*) *distincta* (Dejean, 1831)
M. (*M.*) *smaragdula* (Dejean, 1825)
M. (*M.*) *procera* (Chaudoir, 1860)
M. (*M.*) *proceroides* (Moravec, 2016)
M. (*M.*) *viridis* (Dejean, 1831)

Mesochila (*Neomesochila*), subgen. nov.

http://zoobank.org/6A3DCAC3-1857-4AA6-8A72-0F0C20D-4B50F

Type species. *Odontocheila brevipennis* W. Horn, 1907

Etymology. Composed word formed by *neo* (from Greek, means new) and *Mesochila*, the genus name.

Diagnosis. Smaller body length, usually between 6–9.3 mm; mandibles with four teeth (plus molar one); pronotum as wide as long; elytra 3.3–3.6 times longer than wide, finely punctate; aedeagus thin, with apical third subparallel, with apex forming distinctly wide bent rounded beak, internal sac containing stingray-like ventral spur and an oval feebly sclerotized central sclerite.

4 species included:
- *M.* (*N.*) *brevipennis* (W. Horn, 1907)
- *M.* (*N.*) *drechseli* (Sawada and Wiesner, 1997)
- *M.* (*N.*) *moraveci* (Roza and Mermudes, 2019)
- *M.* (*N.*) *prepusula* (W. Horn, 1907)

Note. It is interesting to point out that the stingray-like ventral spur (term proposed by Moravec 2018a, 2020), one of the most distinct features of *M.* (*Mesochila*), present in almost all species previous to this study, was found to be homoplastic, with independent origins in *M.* (*Neomesochila*) **subgen. nov.** and inside *M.* (*Mesochila*), derived from bifurcate or u-shaped ventral spurs.

Finally, it is important to highlight that the outgroup relationships suggest, in most analysis, a relationship between *Odontocheila nodicornis* and *Phyllodroma lu-*

teomaculata, and in many of them, also between *Pentacomia speculifera* and *Mesachantina chalceola.* As already pointed out by Moravec (2016, 2018a, b, 2020), the *Pentacomia* former subgenera are probably not phylogenetically related, due to several morphological differences. The most conspicuous one is the uniformly shaped protarsi in both sexes in all *Pentacomia* species (unique character in the subtribe and within majority of Cicindelidae). The same goes for *Odontocheila* and *Phyllodroma*, that share an aedeagus flagellum, but with very different morphology and most probably homoplastic (Moravec, 2018b). Only a broader analysis, including representative taxa from all Odontocheilina genera may give better understanding of the group relationships.

4.2. Biogeographic analysis

The S-DIVA analysis presented competing ancestral areas for *Mesochila* and its more internal nodes, many of them with very close probabilities. The results of BMM were more consistent, with most of the more probable areas with high probabilities. This lack of resolution is a common issue in S-DIVA (Kodandaramaiah 2010). We tried to attenuate this bias including the sister group of the focus taxa of the analysis (Ronquist 1997; Kodandaramaiah op. cit.).

This measure, however, seems to have had little effect on the results of this analysis. Even if the results have been more resolved, the sister group of *Mesochila* is unknown. *Pentacomia speculifera* and *Mesacanthina chalceola* were retained in the analysis because they were found as the sister clade of the ingroup in most phylogenetic results. But, as the phylogeny did not have the objective of testing the relationship of Odontocheilina genera, the relationship between *Pentacomia*, *Mesacanthina* and *Mesochila* cannot be trusted. Therefore, any resolved result for the ancestral area of the genus should be taken with caution, at least. However, when comparing both S-DIVA and BMM results, it was clear that the ancestral area was Chacoan dominion, Parana dominion or a composed area of the two. Those dominions encompass Atlantic rainforest, Cerrado and Caatinga biomes.

The recovery of the ancestral split in *M.* (*Paramesochila*), with an ancestral area ADE or with posterior dispersal to this area shows an inedited relationship between the south of Central America and the Atlantic rainforest (In this case, *M. horni* occurs in the Atlantic rainforest biome, sometimes in the border with Caatinga biome). The possible vicariant event here suggests that those two regions were in contact sometime prior to the speciation event between these two lineages. Pleistocenic shifts of vegetation are postulated as a probable cause for the link between Amazon and Atlantic rainforest (Costa 2003; Sobral-Souza 2015), and these shifts may have also connected the northwest Amazon and the Caatinga (De Oliveira et al. 2015). Future studies in the group, with the descriptions of new species with a median distribution between these two areas, may or may not clarify this question.

The recovery of an ancestral area of D, E or DE for the clade B suggests that *M.* (*Mesochila*), *M.* (*Eumesochila*) and *M.* (*Neomesochila*) **subgen. nov.** diversified in these dominions (mainly in Cerrado and Atlantic rainforest), and only recently some species have dispersed to other areas (like Pacific, Boreal Brazilian and South Brazilian dominions, which are mainly covered by tropical wet forests or drier lowland vegetation). Another interesting point is the absence of any species in the South-eastern Amazonian dominion, and almost complete absence in the Caatinga biome (in Chacoan dominion). The amplilocated distribution of *P.* (*M.*) *discrepans* and *P.* (*M.*) *distigma* due to dispersion events may correspond to the hypotheses of Pleistocenic shifts of vegetation that cause a posterior link between Amazon and Atlantic rainforest (Costa 2003; Sobral-Souza 2015). These species could be unable to establish themselves in the above-mentioned areas, or the absence in South-eastern Amazonian dominion and Caatinga may be an artefact of the lack of sampling in those locations.

Finally, as we do not have a hypothesis for the divergence time of the lineages, any cause for these speciations postulated here is merely speculative. Future studies using molecular data can give more insights about the biogeographical events occurring in the history of this group.

5. Acknowledgments

We would like to thank Drs. Ricardo and Margarete Monteiro for the providing many of the malaise samples from Teresópolis and Itatiaia. We would like to thank Instituto Chico Mendes de Conservação da Biodiversidade (ICMBIO) for the authorizations to collect on Nacional Units of Conservation. We are grateful to Jiri Moravec for helping with the identifications, for sending necessary bibliography and for reviewing this manuscript, besides all the help in the studies we perform with Tiger beetles. We also thank the curators that provided access to the visited collections or have sent material for loan during the preparation of this paper: Jane Costa and Ingrid Matos (CEIOC), Norma G. Ganho and Cibele S. Ribeiro-Costa (DZUP); Marcela L. Monné and Miguel A. Monné (MNRJ); Sonia A. Casaria (MZSP); Luciano de A. Moura (MCNZ); Henrique Paprocki (PUCMG); e Simone Rosa (UNIFEI). We thank the Fundação de Amparo à Pesquisa do Estado do Rio de Janeiro (FAPERJ), for the photographic system acquired by through grants: Proc. 110.040/2014; 010.001641/2014 and 111.247/2014. ASR was funded by the Postgraduate program in Zoology at the Museu Nacional, Coordenação de Aperfeiçoamento de Pessoal de Nível Superior – Brasil (CAPES) – Finance Code 001, CNPq 06105/2016-0, and JRMM was funded by CNPq 306105/2016-0 and 311679/2019-6; FAPERJ 211.522/2016.

6. References

Arndt E, Putchkov AV (1997) Phylogenetic investigation of Cicindelidae (Insecta: Coleoptera) using larval morphological characters. Zoologischer Anzeiger 235(3–4): 231–241.

Cassola F, Pearson DL (2000) Global patterns of tiger beetle species richness (Coleoptera: Cicindelidae): their use in conservation

planning. Biological Conservation 95(2): 197–208. https://doi.org/10.1016/S0006-3207(00)00034-3

Costa LP (2003) The historical bridge between the Amazon and the Atlantic Forest of Brazil: A study of molecular phylogeography with small mammals. Journal of Biogeography 30: 71–86. https://doi.org/10.1046/j.1365-2699.2003.00792.x

Duran DP, Gough HM (2020) Validation of tiger beetles as distinct family (Coleoptera: Cicindelidae), review and reclassification of tribal relationships. Systematic Entomology 45(4): 723–729. https://doi.org/10.1111/syen.12440

Duran DP, Moravec J (2013) A new species of the genus *Pentacomia* from Panama (Coleoptera: Cicindelidae). Acta Entomologica Musei Nationalis Pragae 53(1): 49–57. https://www.aemnp.eu/acta-entomologica/volume-53-1/1439/a-new-species-of-the-genus-pentacomia-from-panama-coleoptera-cicindelidae.html

Erwin TL, Pearson DL (2008) A treatise on the Western Hemisphere Caraboidea (Coleoptera), their classification, distributions, and ways of life. Volume II. Carabidae – Nebriiformes 2 – Cicindelitae. Pensoft: Sofia, Bulgaria, 365 pp.

Freitag R (1979) Reclassification, phylogeny and zoogeography of the Australian species of *Cicindela* (Coleoptera: Cicindelidae). Australian Journal of Zoology Supplementary Series 27: 1–99. https://doi.org/10.1071/AJZS066

Giribet G (2003) Stability in phylogenetic formulations and its relationship to nodal support. Systematic Biology 52(4): 554–564. https://doi.org/10.1080/10635150390223730

Goloboff PA (1993) Estimating character weights during tree search. Cladistics 9(1): 83–91. https://doi.org/10.1111/j.1096-0031.1993.tb00209.x

Goloboff PA, Farris JS, Källersjö M, Oxelman B, Ramírez MJ, Szumik CA (2003) Improvements to resampling measures of group support. Cladistics 19(4): 324–332. https://doi.org/10.1111/j.1096-0031.2003.tb00376.x

Goloboff PA, Carpenter JM, Arias JS, Esquivel DRM (2008a) Weighting against homoplasy improves phylogenetic analysis of morphological data sets. Cladistics 24(5): 758–773. https://doi.org/10.1111/j.1096-0031.2008.00209.x

Goloboff PA, Farris JS, Nixon KC (2008b) TNT, a free program for phylogenetic analysis. Cladistics 24(5): 774–786. https://doi.org/10.1111/j.1096-0031.2008.00217.x

Goloboff PA, Torres A, Arias JS (2017) Weighted parsimony outperforms other methods of phylogenetic inference under models appropriate for morphology. Cladistics 34(4): 1–31. https://doi.org/10.1111/cla.12205

Gough HM, Duran DP, Kawahara AY, Toussaint EF (2019) A comprehensive molecular phylogeny of tiger beetles (Coleoptera, Carabidae, Cicindelinae). Systematic Entomology 44(2): 305–321. https://doi.org/10.1111/syen.12324

Gough HM, Allen JM, Toussaint EF, Storer CG, Kawahara AY (2020) Transcriptomics illuminate the phylogenetic backbone of tiger beetles. Biological Journal of the Linnean Society 129(3): 740–751. https://doi.org/10.1093/biolinnean/blz195

Gustafson GT, Baca SM, Alexander AM, Short AE (2020) Phylogenomic analysis of the beetle suborder Adephaga with comparison of tailored and generalized ultraconserved element probe performance. Systematic Entomology 45(3): 552–570. https://doi.org/10.1111/syen.12413

Hoang DT, Chernomor O, von Haeseler A, Minh BQ, Vinh LS (2018) UFBoot2: Improving the ultrafast bootstrap approximation. Molecular Biology and Evolution 35: 518–522. https://doi.org/10.1093/molbev/msx281

Huelsenbeck JP, Ronquist F (2001) MRBAYES: Bayesian inference of phylogenetic trees. Bioinformatics 17(8): 754–755. https://doi.org/10.1093/bioinformatics/17.8.754

Kodandaramaiah U (2010) Use of dispersal–vicariance analysis in biogeography – a critique. Journal of Biogeography 37(1): 3–11. https://doi.org/10.1111/j.1365-2699.2009.02221.x

Lewis PO (2001) A likelihood approach to estimating phylogeny from discrete morphological character data. Systematic biology 50(6): 913–925. https://doi.org/10.1080/106351501753462876

López-López A, Abdul Aziz A, Galián J (2015) Molecular phylogeny and divergence time estimation of *Cosmodela* (Coleoptera: Carabidae: Cicindelinae) tiger beetle species from Southeast Asia. Zoologica Scripta 44(4): 437–445. https://doi.org/10.1111/zsc.12113

López-López A, Vogler AP (2017) The mitogenome phylogeny of Adephaga (Coleoptera). Molecular phylogenetics and evolution 114: 166–174. https://doi.org/10.1016/j.ympev.2017.06.009

Löwenberg-Neto P (2014) Neotropical region: a shapefile of Morrone's (2014) biogeographical regionalisation. Zootaxa 3802(2): 300. https://doi.org/10.11646/zootaxa.3782.1.1

Maddison WP, Maddison DR (2018) Mesquite: a modular system for evolutionary analysis, version 3.40. http://mesquiteproject.org

Mawdsley JR (2009) Taxonomy, ecology, and phylogeny of species of *Lophyra* Motschulsky 1859, subgenus *Eriolophyra* Rivalier 1948 (Coleoptera Cicindelidae). Tropical Zoology 22(1): 57–70.

Mawdsley JR (2011) Taxonomy, identification, and phylogeny of the African and Madagascan species of the tiger beetle genus *Chaetodera* Jeannel 1946 (Coleoptera: Cicindelidae). Insecta Mundi 0191: 1–13. https://journals.flvc.org/mundi/article/view/0191

Mirande JM (2009) Weighted parsimony phylogeny of the family Characidae (Teleostei: Characiformes). Cladistics 25(6): 574–613. https://doi.org/10.1111/j.1096-0031.2009.00262.x

Moravec J (2012) Taxonomic and nomenclatorial revision within the Neotropical genera of the subtribe Odontochilina in a new sense ñ 1. Some changes in taxonomy and nomenclature within the genus *Odontocheila* (Coleoptera: Cicindelidae). Acta Musei Moraviae, Scientiae Biologicae 97(2): 13–33.

Moravec J (2016) Taxonomic and nomenclatorial revision within the Neotropical genera of the subtribe Odontocheilina W. Horn in a new sense — 16. *Pentacomia* (*Mesochila*) *procera* (Chaudoir), *P.* (*M.*) *conformis* (Dejean), and *P.* (*M.*) *proceroides* sp. nov. (Coleoptera: Cicindelidae). Zootaxa 4127(2): 276–300. https://doi.org/10.11646/zootaxa.4127.2.3

Moravec J (2018a) Taxonomic and nomenclatorial revision within the Neotropical genera of the subtribe Odontocheilina W. Horn in a new sense – 20. *Beckerium* W. Horn stat. restit., *Mesochila* Rivalier stat. nov. and *Poecilochila* Rivalier stat. nov. Acta Musei Moraviae, Scientiae Biologicae (Brno) 103(2): 127–206.

Moravec J (2018b) Taxonomic revision of the Neotropical tiger beetle genera of the subtribe Odontocheilina – Volume 1. *Odontocheila* Laporte de Castelnau, *Cenothyla* Rivalier and *Phyllodroma* Lacordaire (Coleoptera: Cicindelidae). Biosférická rezervace Dolni Morava: Lednice na Moravê, Czech Republic, 624 pp.

Moravec, J. (2020). Taxonomic revision of the Neotropical tiger beetle genera of the subtribe Odontocheilina – Volume 2. A complete revision of other twelve genera of the subtribe (Coleoptera: Cicindelidae). Biosférická rezervace Dolni Morava: Lednice na Moravê, Czech Republic, 592 pp.

Moravec J, Brzoska D (2013) Taxonomic and nomenclatorial revision within the Neotropical genera of a subtribe Odontochilina W. Horn in a new sense – 5. A new species of the genus *Pentacomia* from Costa Rica (Coleoptera: Cicindelidae). Acta Musei Moraviae, Scientiae biologicae (Brno) 98(1): 75–84.

Moravec J, Brzoska D (2014) Taxonomic and nomenclatorial revision within the Neotropical genera of the subtribe Odontocheilina W. Horn in a new sense œ 7. *Pentacomia* (*Pentacomia*) *davidpearsoni* sp. nov., a new species from Bolivia related to *P.* (*P.*) *speculifera* (Brullé) (Coleoptera: Cicindelidae). Acta Musei Moraviae, Scientiae biologicae (Brno) 99(1): 15–33.

Moravec J, Huber RL (2015) Taxonomic and nomenclatorial revision within the Neotropical genera of the subtribe Odontocheilina W. Horn in a new sense œ 13. The genus *Mesacanthina* Rivalier, stat. nov., separated from the genus *Pentacomia* Bates (Coleoptera: Cicindelidae). Acta Musei Moraviae, Scientiae biologicae (Brno) 100(1): 67–114.

Morrone JJ (2014) Biogeographical regionalisation of the Neotropical region. Zootaxa 3782(1): 1–110. https://doi.org/10.11646/zootaxa.3782.1.1

Minh BQ, Nguyen MAT, von Haeseler A (2013) Ultrafast approximation for phylogenetic bootstrap. Molecular biology and evolution 30(5): 1188–1195. https://doi.org/10.1093/molbev/mst024

Nixon KC (2002) WinClada ver. 1.00. 08. Ithaca, NY.

Nguyen LT, Schmidt HA, von Haeseler A, Minh BQ (2015) IQ-TREE: A fast and effective stochastic algorithm for estimating maximum likelihood phylogenies. Molecular Biology and Evolution 32: 268–274. https://doi.org/10.1093/molbev/msu300

De Oliveira PE, Barreto AMF, Suguio K (1999) Late Pleistocene/Holocene climatic and vegetational history of the Brazilian caatinga: the fossil dunes of the middle São Francisco River. Palaeogeography, palaeoclimatology, palaeoecology 152(3–4): 319–337. https://doi.org/10.1016/S0031-0182(99)00061-9

O'reilly JE, Puttick MN, Pisani D, Donoghue PCJ (2018) Probabilistic methods surpass parsimony when assessing clade support in phylogenetic analyses of discrete morphological data. Palaeontology 61(1): 105–118. https://doi.org/10.1111/pala.12330

Pearson DL (1988) Biology of tiger beetles. Annual Review of Entomology 33: 123–147. https://doi.org/10.1146/annurev.en.33.010188.001011

Pearson DL, Guerra JF, Brzoska DW (1999) The tiger beetles of Bolivia: their identification, distribution and natural history (Coleoptera: Cicindelidae). Contributions on Entomology, International 3: 381–523.

Pearson DL, Vogler AP (2001) The evolution, ecology and diversity of the cicindelids. tiger beetles. Comstock Publishing Associates, Cornell University Press: New York, USA, 352 pp.

Puttick MN, O'reilly JE, Tanner AR, Fleming JF, Clark J, Holloway L, Lozano-Fernandez J, Parry LA, Tarver JE, Pisani D, Donoghue PCJ (2017) Uncertain-tree: discriminating among competing approaches to the phylogenetic analysis of phenotype data. Proceedings of the Royal Society B 284: 1–9. https://doi.org/10.1098/rspb.2016.2290

QGIS Development Team (2016) QGIS Geographic Information System. Open Source Geospatial Foundation Project. http://www.qgis.org/en/site/index.html

Rivalier E (1969) Démembrement du genre *Odontochila* [col. Cicindelidae] et révision des principales espèces. Annales de la Societe entomologique de France (N.S.) 5(1): 195–297.

Ronquist F (1997) Dispersal–vicariance analysis: a new approach to the quantification of historical biogeography. Systematic Biology 46: 195–203.

Ronquist F, Huelsenbeck JP (2003) MrBayes3: Bayesian phylogenetic inference undermixed models. Bioinformatics 19: 1572–1574. https://doi.org/10.1093/bioinformatics/btg180

Roza AS, Mermudes JRM (2017) Distribution of *Pentacomia* (*Mesochila*) Rivalier, 1969 (Coleoptera: Carabidae, Cicindelinae). Transactions of the American Entomological Society 143(3): 601–623. https://doi.org/10.3157/061.143.0305

Sawada H, Wiesner J (1997) Zwei neue Cicindelidae aus Paraguay (Coleoptera). Entomologische Zeitschrift mit Insektenbörse 107: 127–132.

Sereno PC (2007) Logical basis for morphological characters in phylogenetics. Cladistics 23(6): 565–587. https://doi.org/10.1111/j.1096-0031.2007.00161.x

Serrano ARM (2000) Are tiger beetles (Coleoptera: Cicindelidae) well studied? A myth or a reality? In: Sobti RC, Yadav J (Eds) Some Aspects on the Insight of Insect Biology Narendra Publishing House: Delhi, India, 69–90.

Sobral-Souza T, Lima-Ribeiro MS, Solferini VN (2015) Biogeography of Neotropical rainforests: past connections between Amazon and Atlantic forest detected by ecological niche modelling. Evolutionary Ecology 29(5): 643–655. https://doi.org/10.1007/s10682-015-9780-9

Trifinopoulos J, Nguyen LT, von Haeseler A, Minh BQ (2016) W-IQ-TREE: a fast online phylogenetic tool for maximum likelihood analysis. Nucleic Acids Research 44(1):232–235. https://doi.org/10.1093/nar/gkw256

Vogler AP, Pearson DL (1996) A molecular phylogeny of the tiger beetles (Cicindelidae): congruence of mitochondrial and nuclear rDNA data sets. Molecular Phylogenetics and Evolution 6(3): 321–338. https://doi.org/10.1006/mpev.1996.0083

Wiesner J (2020) Checklist of the Tiger Beetles of the World (2nd Edition). Winterwork: Borsdorf, Germany, 520 pp.

Wright AM, Hillis DM (2014) Bayesian analysis using a simple likelihood model outperforms parsimony for estimation of phylogeny from discrete morphological data. PLoS One 9(10): e109210. https://doi.org/10.1371/journal.pone.0109210

Yu Y, Harris AJ, He X (2010) S-DIVA (Statistical Dispersal-Vicariance Analysis): a tool for inferring biogeographic histories. Molecular Phylogenetics and Evolution 56(2): 848–850. https://doi.org/10.1016/j.ympev.2010.04.011

Yu Y, Harris AJ, Blair C, He X (2015) RASP (Reconstruct Ancestral State in Phylogenies): a tool for historical biogeography. Molecular phylogenetics and evolution 87: 46–49. https://doi.org/10.1016/j.ympev.2015.03.008

Zerm M, Wiesner J, Ledezma J, Brzoska D, Drechsel U, Cicchino AC, Rodríguez JP, Martinsen L, Adis J, Bachmann L (2007) Molecular phylogeny of Megacephalina Horn, 1910 tiger beetles (Coleoptera: Cicindelidae). Studies on Neotropical Fauna and Environment 42(3): 211–219. https://doi.org/10.1080/01650520701409235

Supplementary material 1

Appendix S1

Authors: Silva Roza A, Schrago C, Mermudes JR (2022)
Data type: .docx
Explanation note: Material examined for each terminal of the phylogenetic analysis.

Link: https://doi.org/10.3897/asp.80.e76575.suppl1

Supplementary material 2

Table S1

Authors: Silva Roza A, Schrago C, Mermudes JR (2022)
Data type: .pdf
Explanation note: Matrix of terminals and characters.

Link: https://doi.org/10.3897/asp.80.e76575.suppl2